EXPLORING THE ROLE OF THE STRINGENT RESPONSE IN *MYCOBACTERIUM TUBERCULOSIS* DORMANCY

by
Alysha L. Ellison

A thesis submitted to Johns Hopkins University in conformity with the requirements for the degree of Master of Science

Baltimore, Maryland

May, 2018

Abstract

Mycobacterium tuberculosis is the leading cause of death by an infectious disease and remains one of the top overall causes of mortality worldwide. With antibiotic resistance rising and persistence an impending threat, research into mechanisms of antibiotic tolerance is pertinent. The stringent response is responsible for decreased replication and a reduced metabolic state in stressed conditions, a physiological state that is thought to be a major contributor to latent tuberculosis infection and the lengthy duration of treatment for tuberculosis. The Rel_{Mtb} enzyme regulates accumulation of the stringent response effector molecule, (p)ppGpp. It is hypothesized that learning to control this enzyme may allow modulation of the *M. tuberculosis* stringent response, potentially leading to a better understanding of antibiotic tolerance and immune evasion, as well as new methods of treating tuberculosis. To learn more about this pathway and deduce whether or not accumulation of (p)ppGpp is sufficient to induce the stringent response. We have generated a conditional Rel_{Mtb} overexpression strain by molecular cloning techniques that lacks the ability to hydrolyze (p)ppGpp. This strain responds to an anhydrotetracycline inducing agent by increasing expression of the gene of interest. Inducible expression at the genetic and protein level has been confirmed, but more time and data are needed to characterize this strain and determine the actual effects on (p)ppGpp and the stringent response.

Primary Advisor: Dr. Petros Karakousis

Secondary Advisor: Dr. Douglas Norris

Acknowledgements

In the course of my graduate studies at Johns Hopkins University, countless individuals have guided me through mentoring and sharing advice, as well as supporting and encouraging me. Without them, none of what has been accomplished would have been possible. The multitude of people deserving of recognition is far beyond the pages of this thesis, but I wish to attempt to acknowledge a few of the many who have impacted my time as a master's student.

Initial thanks must be given to the Department of Molecular Microbiology and Immunology for accepting me into the Master of Science program. Two years ago, I felt applying to the program was a leap of faith into a giant chasm, but I am so glad I did. Thank you for catching me and showing me that what I perceived to be a chasm was in reality a phenomenal opportunity. During my time spent in this department I have gained a multitude of new experiences, and am perpetually inspired by the community of scientists I am fortunate enough to call colleagues. Additional recognition must be extended to the Center for Tuberculosis Research for providing a place to conduct my thesis research, and a network of talented mentors and colleagues to work with and learn from. I would also like to acknowledge the funding sources that have made this thesis project possible, including two grants from the National Institutes of Health (R21AI122922 and R21AI114507) and the Emergent BioSolutions Fellowship from Emergent BioSolutions Incorporated.

Many thanks must be given to my primary thesis advisor, Dr. Petros Karakousis. I appreciate his willingness to accept a master's student without a TB background in his lab and his patience as I have attempted to learn a new field and project. This thesis would not have been possible without Petros's support and guidance as I have grown into the TB field. He constantly challenges me to think critically and broaden my perspective and I continually learn something new from each of our conversations. The depth and breadth of his knowledge in the

TB field and beyond knows no bounds and matches, with equal measure, his generosity in all aspects. Petros readily offers his time to answer questions, considers different viewpoints with genuine interest, and has graciously allowed me time away from the lab when it has been most important. Enough appreciation cannot be expressed for his willingness to partake in meaningful discussions, as well as his understanding and flexibility. I am truly thankful for the opportunity to have completed my thesis in the Karakousis lab, and for a mentor whom I admire and respect enough to emulate.

I am exceedingly grateful to my secondary thesis advisor, Dr. Douglas Norris, for agreeing to serve as my second advisor and reader. He has provided relevant feedback for every question I've asked and never ceases to make time for me in what I know is a very busy schedule. I appreciate his advice as I navigate the rigors of the ScM program and in all matters thesis related. Dr. Norris is always ready with an encouraging comment and has the remarkable ability to know the exact words I need to hear, reminding me to redirect my focus on the most important goals and that patience is key. His reassurance in moments of uncertainty has been immeasurably helpful and I cannot thank him enough for all he has done to enable my continued success at Johns Hopkins.

I would also like to recognize and thank Dr. Yu-min Chuang for sharing his knowledge on the Rel project and helping me begin the initial studies for my thesis despite his many additional obligations. In addition, creation of the various strains for this project would not have been possible without the assistance of Dr. Korin Bullen, who generously took time from her busy schedule to instruct me on the theory and details of subcloning. Dr. Pankaj Kumar also deserves acknowledgement for showing me the process of protein purification and taking the time to answer my many questions during the troubleshooting of this process.

My sincere gratitude goes to William Matern for being generous with his time in answering a profuse amount of questions and patiently explaining concepts as many times as needed for me to understand them. To the rest of the Karakousis lab, Michael Pinn, Dr. Noton Dutta, Dr. Victoria Campodónico, and Monika Looney, thank you for sharing the highs and lows that come with every master's thesis. I value and have thoroughly enjoyed our many conversations, from how to process leukopaks and the pros and cons of pursing a PhD to who won the Ravens game and the significance of mate tea. I am also grateful to Dr. Laurene Cheung for her advice on a variety of topics throughout my time at Johns Hopkins, as well as Stefanie Krug for her vibrant friendship and perspective when I need it most. In addition, Dr. Michael Urbanowski has been especially helpful in allowing me to borrow from his collection of TB related books and facilitating a better understanding tuberculosis pathology.

Surviving the first year of classes would have been infinitely more difficult if not for the kind support of Kristin Poti. As a senior student in the department, her advice and reassurance that we would all make it through the typical first-year challenges is much appreciated. I am also grateful for our experiences as roommates, which never fail to keep life interesting. Flaming pots of doom and midnight fire department calls because of random carbon monoxide alarms are no match for weekend ice cream runs and I am so glad to have shared in these memories. To the Brunch Brigade! Madhura Kulkarni, Tanvi Potluri, and Hebe Rosado Rivera, thank you for exploring Baltimore with me and being willing to try different restaurants, embark on crazy adventures, and keeping me sane during the past two years. Struggling through classes, figuring out labs, and navigating thesis work and writing would have been impossible without you. I am so glad we have become friends and struggled through this process together. Thank you for everything.

My acknowledgements would not be complete without recognizing the superb staff I have had the pleasure of interacting with during the course of my thesis work. Ms. Gail O'Connor is the queen of making sure the graduate students have everything we need, and has an answer for every question we ask, no matter how many times we ask it. Scientists are trained to tell you there is always a scientific explanation behind the mystical, but the wizardry Gail performs every day is nothing short of magic. I must also thank Payne, all of the shuttle drivers, walking escorts, and the entire Transportation Department staff, as well as Alberto Saavedra, Norma Thomas, and Ansu Bafalie. These individuals, with whom I have been fortunate enough to share some of the most poignant conversations, are a constant source of support, encouragement, and perspective. They ensure I arrive home safely following long nights in the lab, help keep me grounded in the priorities that are important, and remind me to continue striving for my goals.

I owe an immense debt of gratitude to Dr. James Perfield for seeing beyond the student I was to the scientist I could become, and without whose encouragement I would never have had the courage to apply to the master's program at Johns Hopkins. I am also exceedingly grateful to Dr. Ricardo Samms for his endless stream of advice and never missing a chance to remind me to believe in myself. His determination and words of encouragement will not soon be forgotten. Additionally, I wish to acknowledge and thank Dr. John McKillip for giving me a place in his lab as an undergraduate student who did not even know how to hold a pipette, and initiating my journey into the wonderful world of microbiology and research. I knew absolutely nothing when I entered the lab except that I loved every new aspect I learned about. And by the time I graduated with my bachelor's degree, I could not imagine a life without microorganisms and research. Many thanks are also in order to Mr. Bill Mahoney, Mrs. Denise Stephenson, Mrs. Amy Miller, Mr. Michael Dodrill, and especially Mrs. Nancy Watson for laying the foundation of

my scientific interest throughout my primary and secondary education. I would also like to express my deepest appreciation for Dr. Timothy Berg and his ability to inspire an openness to new perspectives and ideas I had never encountered before. He unwittingly introduced me to the text that would help shape and direct my passion for people into what has ultimately become a focus on public health.

It goes without saying that my family has taken this journey with me and deserves my utmost gratitude for their unwavering support during the past two years and throughout my life. Thank you to my Mom for teaching me to always do my best, no matter what, and being the model from which I learned the rigorous work ethic that has served me so well. I cannot express enough gratitude for her indefatigable belief in my ability to succeed, her steadfast concern for what is best for me, and, without fail, perfect timing on the best care packages in Baltimore. Thank you to my Dad for teaching me the importance of being organized and disciplined in every task I undertake and for his unrelenting edification (and also for the gift of sarcasm and putting up with my sass for many years). Thank you to my brother, Isaac, for being the best friend in the world and always making me laugh. My cat, Jenny, is also deserving of an abundance of thank-yous. She has been my constant companion, from moving halfway across the United States with me to late nights of studying and TV show marathons. She never misses a chance to keep me company and is always waiting to greet me no matter how late I come home from the lab.

I would be remiss if I did not also thank my extended family for growing up with me and helping to build the foundation for who I am today. I love you all. Grandma Faye for quilts that always keep you warm no matter how cold the winter wind and Uncle Darrell for reminding me how important it is to care. My grandparents for sherbet in the afternoons after school, snickerdoodles and scrabble on long summer days, walks around the block and to the park, and

just enough teasing to put me in my place. And finally, to LJO, my exceptional grandmother, thank you for teaching me the art of bringing people together with food and the value of stopping to listen. I am forever indebted to you for the gift of sending me on one of the toughest, but most meaningful, detours of my life.

All that in idea seemed simple became in practice immediately complex | Virginia Woolf

Table of Contents

Tables

Figures

Introduction

Tuberculosis

Phthisis (φθίσης), meaning "wasting", and "consumption" were commonly used to describe pulmonary tuberculosis (TB) for many years. Johann Schoenlein, however, is credited with formally establishing the current name of the disease in 1839, based on the tuber, or potato-like structure, found on gross examination of diseased organs (Figure 1). While TB likely affected humans before, it is first described in detailed records in ancient Greece, with references in the Hippocratic Collection [1]. Widespread for numerous years and consistently in the top three causes of death in the United States until the 1920's [2], TB has claimed the lives of many world-renowned historical figures, including Frédéric Chopin, John Keats, and the Brontë sisters (Charlotte, Emily, and Anne) [3]. Among the scientists and physicians who succumbed to TB because of their dedication to its study are French physicians Gaspard Bayle and René Laennec, whose discovery of the stethoscope endures as a trademark tool of medical doctors today. TB remained one of the top ten causes of death worldwide in 2016 [4], with 1.7 million people dying of the disease and almost one third of these deaths occurring in people affected by HIV/TB coinfection [4]. In addition, the greatest incidence of TB cases annually is in sub-Saharan Africa and southeast Asia. With antibiotic resistance, multi-drug resistant TB (MDR-TB), and extremely drug resistant TB (XDR-TB) on the rise, one in five people receiving the MDR-TB treatment they need, and the issues of latent TB infection and persistence looming, much work is to be done if the World Health Organization (WHO) goal of eliminating TB by 2030 is to be achieved [4,5].

Past treatments for TB include everything from fasting and exorcisms to horseback riding and the practices of bleeding and purging popular into the 19th century. In 1859, German physician Hermann Brehmer formally introduced the idea of the sanatorium, a retreat for

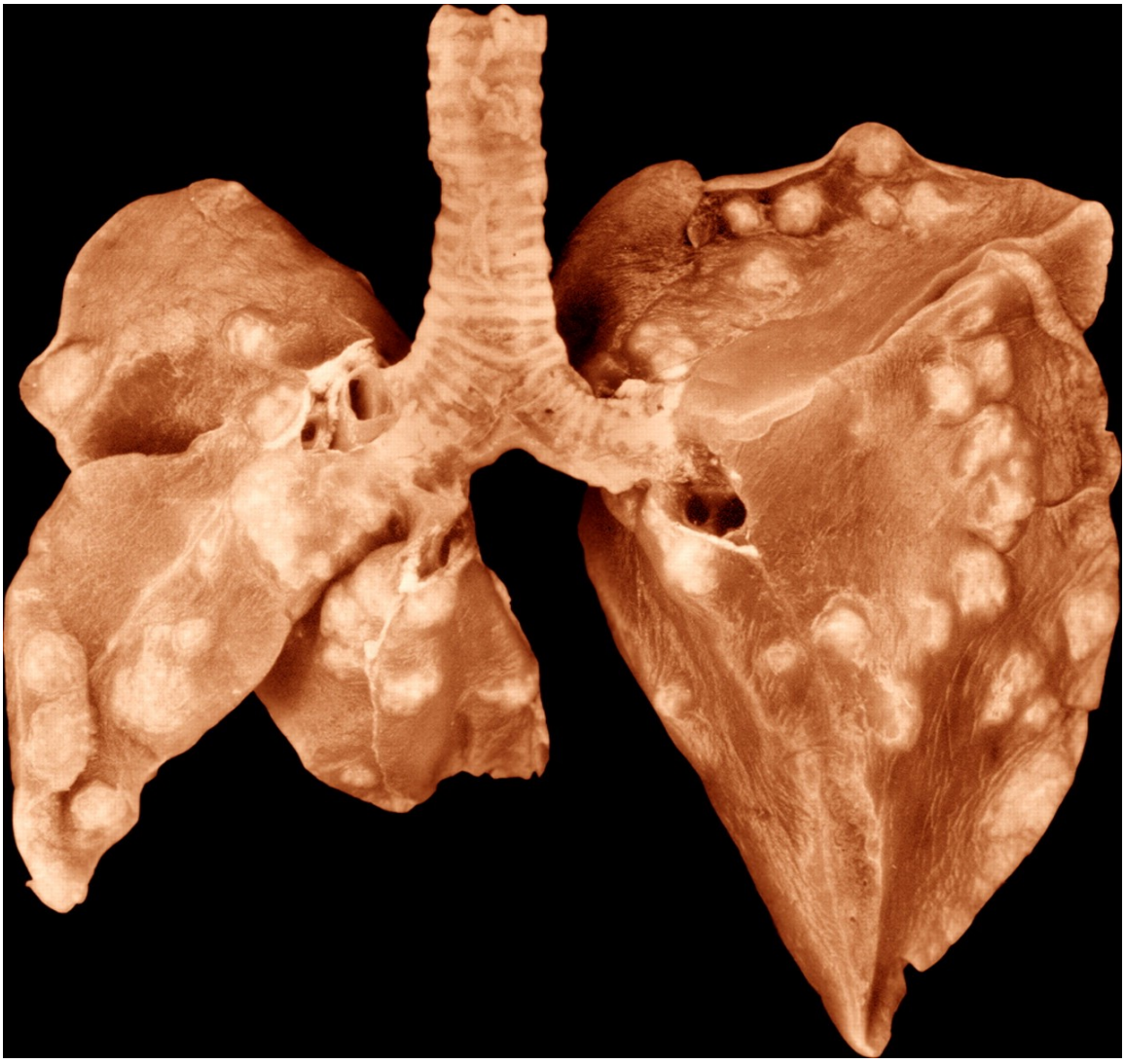

Figure 1 Gross pathology of tuberculosis Posterior view of New Zealand white rabbit lungs affected by tuberculosis. At 5 weeks post infection numerous tubercles or tubers, swollen, potato-like structures, can be seen, and were the basis for Johann Schoenlein's naming of the disease [72].

tuberculous patients, where exposure to fresh air, rest, and a nutritious diet, along with supervised medical care, was said to allow the lungs to recover. Patient populations in sanitoria rose from just under 12,000 in 1908 to more than 90,000 in 1942, providing an ideal environment for introduction of collapse therapy. In its most basic form, collapse therapy was contraction of the lung into an uninflated state by various mechanisms to allow it to heal, with incorporation of a number of refinements over time before the advent of chemotherapy. Among the first antibiotics developed to treat TB were para-amino salicylate, streptomycin, and

isonicotinic acid hydrazide, the latter of which remains a critical component of current anti-TB therapy as the derivative isoniazid [1]. With the emergence of HIV in the 1980's and the WHO's declaration of TB resurgence as a global health emergency in 1993, focus on a new strategy was needed. The current first-line treatment regimen for antibiotic sensitive TB employs combination therapy utilizing rifampin, isoniazid, ethambutol, and pyrazinamide for six to nine months. In addition, introduction of directly observed therapy, short course (DOTS) has helped ensure patients complete the course of treatment, and aids in preventing antibiotic resistance [6]. However, treatment of MDR-TB requires at least 18 months of treatment with antibiotics that are less effective, more costly, and more toxic. With the emergence of XDR-TB, treatment options have become even more limited. Patients and physicians are forced to combat XDR-TB using an ever shrinking list of antibiotics with a concomitantly growing list of side effects, leaving a narrow therapeutic margin between eradicating the infection and harming the patient [7].

Numerous philosophers and scientist have made predictions through the years about the type of disease TB is, and what might be the cause of such a devastating disease. Though he had no rigorously validated evidence, Aristotle postulated that TB is spread from person to person by a disease producing agent in the air breathed by people affected with the disease. The Greek physician Aretaeus also noted and described in great detail the various clinical manifestations of chronic TB [1]. Franciscus de la Boe, better known as Sylvius, observed nodules in the organs of TB patients upon autopsy and asserted that these tubercles, or swellings, are the precursor to cavities. Because of this finding, he and his peers were able to differentiate TB from other wasting diseases. Pierre Desult later suggested these tubercle structures develop as a direct result of TB, a hypothesis confirmed by William Stark and Matthew Baillie in the course of conducting autopsies that showed tubercles arise and progress to cavities in response to TB disease [1]. Also known for his work with post-mortem TB cases,

Gaspard Bayle chronicled detailed patient histories, allowing immense leaps forward in piecing together clinicopathological correlations [1]. Confirming some theories about the cause of TB and quashing others, Robert Koch's discovery of the etiological agent of TB in 1882 proved a momentous event in history [8]. Not only was Koch able to culture and view the tubercle bacillus, he proved a causal relationship between the bacillus, named *Mycobacterium tuberculosis*, and TB disease, developing his famed Koch's Postulates in the process. He also experimentally validated the idea that transmission occurs from one human to another via cavitation in the lungs based on visualization of the tubercle bacillus in sputum from human TB patients [1,8].

Mycobacterium tuberculosis infection

The causative agent of tuberculosis (TB), *Mycobacterium tuberculosis*, is a Gram positive, acid-fast, rod-like organism [9] that primarily infects human lung tissue, but is able to disseminate to other organs [10]. *M. tuberculosis* enters the human body by inhalation of infectious aerosol particles and passes into the alveoli of the lungs. The classical theory of *M. tuberculosis* infection postulates that resident alveolar macrophages engulf the bacterium through the process of phagocytosis, confining *M. tuberculosis* to a phagosome within the macrophage. Depending on their activation state, some macrophages are able to immediately kill the engulfed bacteria. Others do not have the capacity to do so and become a haven for bacterial multiplication [11]. Two subsets of macrophages, active and naïve, participate in the initial response against *M. tuberculosis* infection. Activated macrophages follow the normal process of phagosome maturation, where a phagosome containing the bacterium fuses with a lysosome containing hydrolytic enzymes that break down various biomolecules. Thus, *M. tuberculosis* is degraded and killed in the phagolysosome before multiplying and infecting

additional immune cells. However, when *M. tuberculosis* infects naïve macrophages, the bacteria have evolved to circumvent the process of phagosome maturation, preventing the acidic pH change necessary for phagolysosomal fusion and bacterial degradation [12]. Consequently, the bacteria can continue to multiply within the macrophage phagosome, eventually causing death by apoptosis or necrosis [13], or enter into a dormant state to evade immune and antibiotic pressure. Regardless, all infected macrophages produce cytokines that recruit additional mononuclear immune cells from surrounding blood vessels to the tissue. These immune cells, along with proliferating bacteria, form the early structure of the traditional tuberculous granuloma. As granuloma formation progresses, established cells begin to exhibit a range of differing phenotypes, including lipid-rich foam cells, macrophages displaying epithelioid

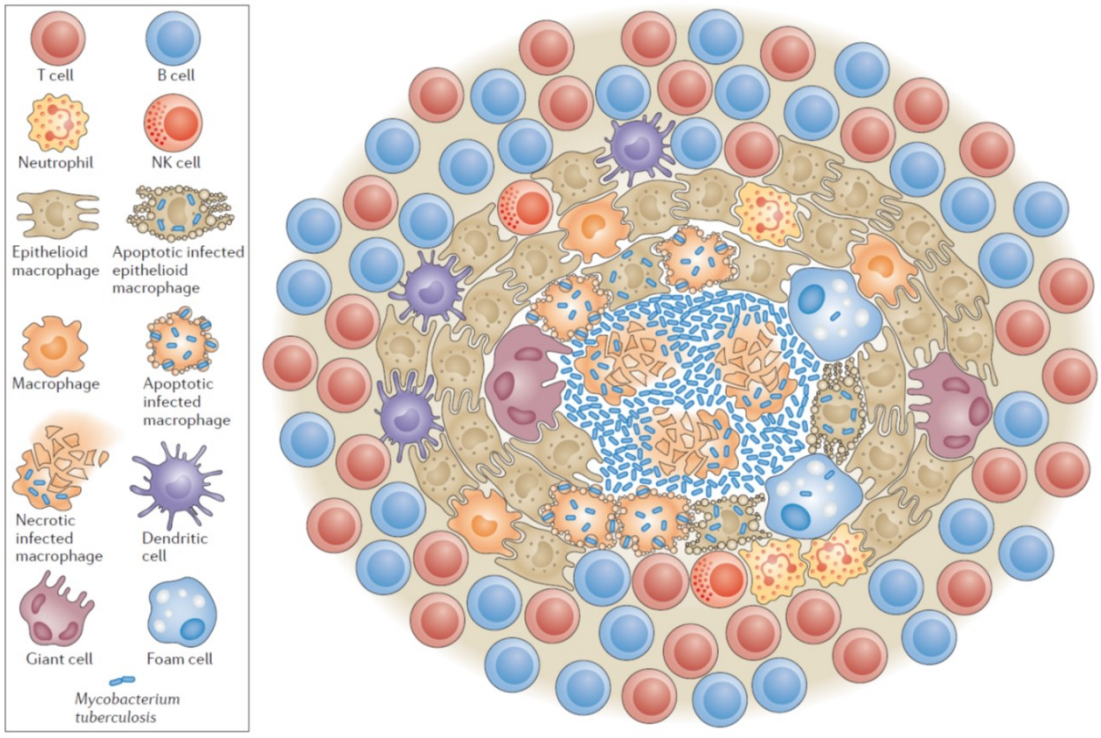

Figure 2 Cellular contents of the necrotic granuloma At the center of the necrotic granuloma are M. tuberculosis bacteria and infected, dying macrophages that, together, comprise the caseum. Additional granulomatous layers surrounding the necrotic center mostly consist of modified cell types, such as foam cells, epithelioid macrophages, and multinucleated giant cells. Other immune cells, including natural killer (NK) cells, neutrophils, and dendritic cells are also found throughout the granuloma. Adaptive immune cells, however, usually remain at the edges and are traditionally thought to be precluded from leaving the granuloma by a fibrous cuff that forms as part of the maturation process [13].

characteristics, multinucleated giant cells, and various forms of cell death [13] (Figure 2). Bacterial replication decreases as the vasculature of the infected tissue recedes, new lymphocytic cells are recruited, and a fibrous cuff begins to form around the granuloma core. This fibrotic edge excludes many lymphocytes from the granulomatous structure, but is thought to contain and prevent spread of bacteria to other parts of the lung [14]. However, recent studies are beginning to challenge this paradigm by showing infected cells are capable of crossing the fibrotic capsule and migrating out of the granuloma [13,15-17]. Dying cells within the granuloma often undergo caseous necrosis that leads to cellular fragmentation and degradation, giving rise to the so called caseum at the center of the granuloma and its

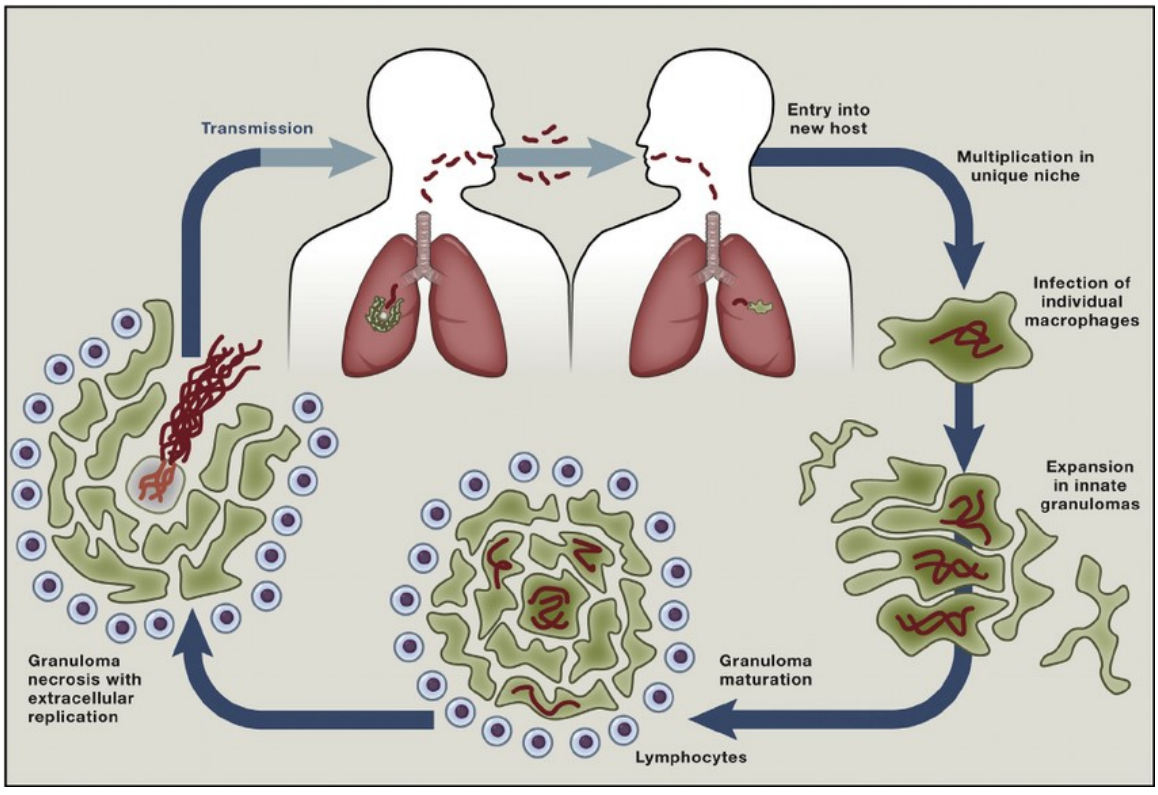

Figure 3 *Mycobacterium tuberculosis* infection *M. tuberculosis* enters the human body by inhalation through the airways and passes into the alveoli of the lungs. Here it infects macrophages, succumbing to immune mediated killing or evading degradation by circumventing the pH change that takes place. Cytokines produced by infected macrophages recruit additional immune cells, which begin to form the early structure of a granuloma. Debris left in the wake of dying cells within a maturing granuloma give rise to the caseum, which either hardens to form a permanent tubercle or softens and liquefies. These liquefied contents are expelled from the lungs upon coughing, leaving a hollow cavity exposed to the airways. This open access to the outside air is an ideal environment for *M. tuberculosis* replication, dissemination, and transmission to other individuals, continuing the cycle of disease [76].

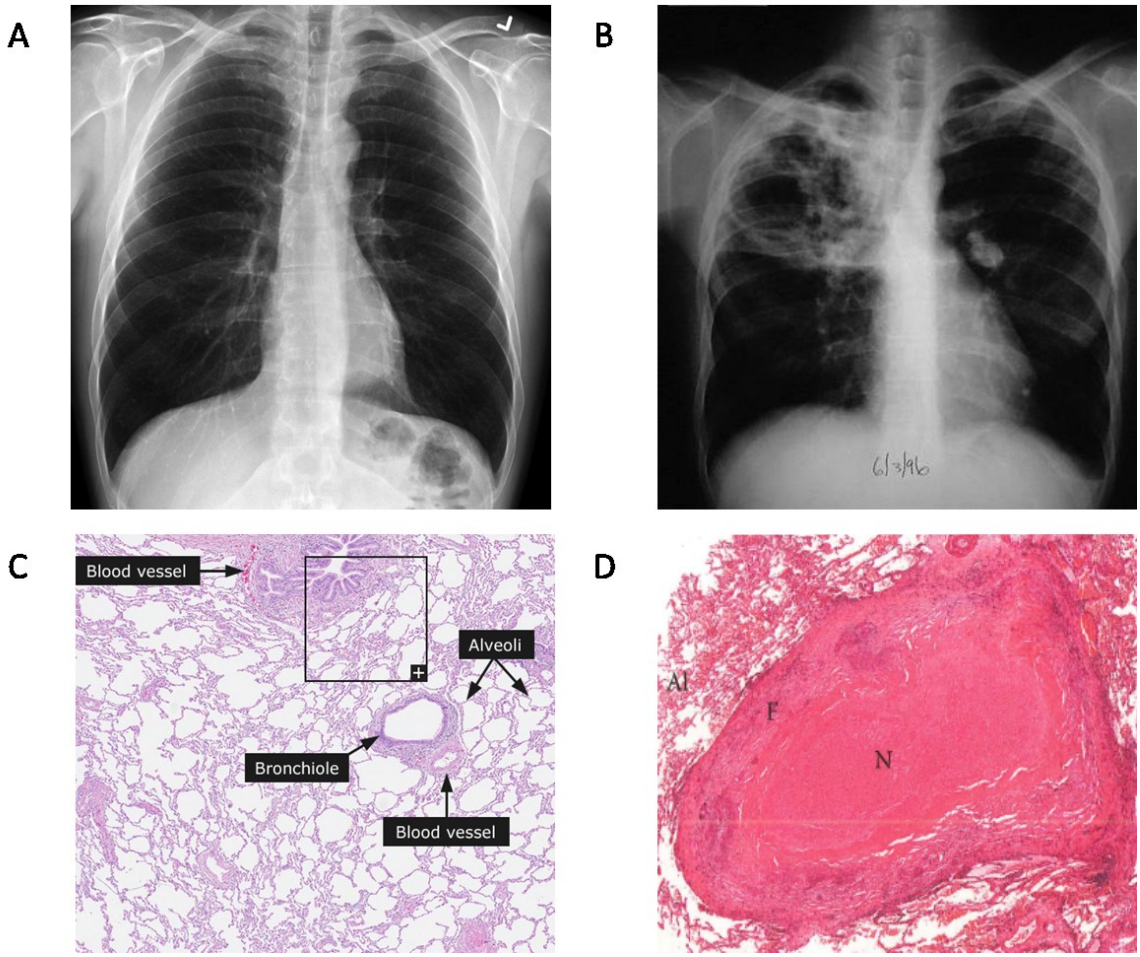

Figure 4 Comparison of normal and diseased lungs Radiographic and histological comparison of human lungs in individuals without (A, C) and with (B, D) tuberculosis. A) Normal chest X-ray with dark regions indicating normal, air-filled lung tissue [71]. B) Abnormal chest X-ray with white opacity in the upper right lobe (left side of X-ray) characteristic of lung disease. The dark circular region within the white opacity signifies an open space and correlates with cavitation, strongly suggesting TB disease [74]. C) Histologically normal lung tissue. H&E staining reveals blood vessels, a bronchiole, and normal alveoli with ample space for exchange of oxygen [75]. D) Histologically abnormal lung tissue with H&E staining showing the fibrotic wall (F) and necrotic center (N) of a granuloma. These formations take the place of air in the alveolar space (Al), damage delicate structures, and reduce the area available for oxygen exchange[77].

characteristic cottage cheese-like appearance [14]. Due to currently unknown stimuli within the granuloma microenvironment, the caseum either hardens or softens. Hardening of the caseum is associated with a lower bacterial burden, whereas a plethora of bacteria are commonly seen in softening caseum [13]. With a lack of bacterial control and disease progression the caseum liquefies and is expelled from the lungs, leaving a hole visible by chest X-ray (Figure 4) where there was previously healthy lung tissue. This cavitation provides a prime environment for extracellular bacterial replication and connects what was once the granuloma's center to the

airways of the lungs. Coughing due to irritation from damaged lung tissue disseminates bacteria into the outside air, exposing surrounding individuals to infectious aerosol particles that can be viable for several hours and perpetuating the cycle of disease (Figure 3) [14].

Mycobacterium tuberculosis resistance, persistence, and latent TB infection

Antibiotic susceptible TB is treatable utilizing 6 to 9 months of therapy involving a combination of different antibiotics. However, disease caused by antibiotic resistant strains of *M. tuberculosis* requires a minimum of 18 months of therapy with multiple antibiotics, which are less effective, more costly, and more toxic than those in the standard first-line regimen [7]. These resistant bacteria contain genetic mutations or acquire extra genes through horizontal gene transfer that allow them to thrive despite antibiotic pressure typically sufficient to kill bacteria [18]. However, persistence and antibiotic tolerance are defined by different qualities than those characteristic of antibiotic resistance. The physiological state of ceased replication and reduced metabolism in the presence of antibiotic pressure has been identified as persistence, and bacteria capable of undergoing this process are often tolerant to antibiotics. This antibiotic tolerance is characterized by survival of prolonged exposure to antibiotics, despite continued susceptibility to inhibition at the minimum inhibitory concentration. However, these changes are non-heritable and if antibiotic pressure is removed, descendants of antibiotic tolerant bacteria are susceptible to killing by antibiotics [19,20]. Persistent bacteria are more difficult to target than actively replicating *M. tuberculosis*, as the majority of first-line treatments, such as isoniazid, interfere with cell wall metabolism or otherwise require active replication to be effective. Pyrazinamide and rifampin are the primary antibiotics targeting nonreplicating, persistent *M. tuberculosis* [21]. This nonreplicating population of bacteria is thought to contribute to the prolonged duration of TB treatment, and to comprise the

population of *M. tuberculosis* responsible for infection without clinical symptoms or radiographic evidence of disease, termed latent TB infection (LTBI) [21,22].

An estimated one third of the world's population is latently infected with *M. tuberculosis* [4]. Though it is difficult to provide concrete proof of the physiological and metabolic state of *M. tuberculosis* during LTBI due to the inability to isolate bacteria during this phase of disease, various tissues, including adipose depots [23], from individuals who died of causes other than TB have been found to harbor *M. tuberculosis* [24]. In addition, lymph node material from individuals negative for TB disease upon gross and histological examination postmortem is cultivable for *M. tuberculosis*, indicating humans can be infected with viable *M. tuberculosis* in the absence of clinical and pathological evidence of disease and that the supposed quiescent state of these bacteria is reversible [25,26]. The ability of *M. tuberculosis* to be resuscitated in the absence of immune or antibiotic pressure creates bacterial populations fully capable of replicating and dividing and introduces the possibility of reactivation of disease many years after infection [27]. This reactivation perpetuates the cycle of disease, forming a barrier to TB elimination. As such, a better understanding of LTBI and persistence is essential in accomplishing the goal of eliminating TB and protecting the world's populations from disease. Because the bacterial phenotypes during LTBI and persistence may be similar, learning about one may serve to elucidate knowledge about the other. In this line of thinking, researchers are studying mechanisms of growth restriction and metabolic control. One such mechanism is the stringent response, a complex pathway necessary for extended survival of many bacteria, including *M. tuberculosis* [28].

The stringent response

The stringent response is one method by which both Gram-positive and Gram-negative bacteria [29,30], as well as plants [31], respond to varying types of stress. In these organisms, the stringent response is largely mediated by hyperphosphorylated guanosine, an alarmone signal that alerts the cell to adverse conditions. This molecule is synthesized in various bacteria by the key stringent response factor Rel and its homologs. The enzyme transfers two terminal phosphates from ATP to GTP or GDP, forming two different molecules termed pentaphosphorylated guanosine (pppGpp) or tetraphosphorylated guanosine (ppGpp), respectively, and collectively referred to as hyperphosphorylated guanosine [(p)ppGpp] [29]. These molecules are hydrolyzed to GTP or GDP and inorganic pyrophosphate (PP_i) [32] by SpoT homologs, maintaining a balance of (p)ppGpp and ensuring adequate cellular homeostasis when conditions are optimal (Figure 5A). However, bacteria experiencing nutrient restriction accumulate (p)ppGpp (Figure 5B) and, when the alarmone reaches sufficient levels, the stringent response is triggered [33]. Resulting physiological changes lead to a slowly replicating, persistent phenotype characterized by disrupted RNA polymerase (RNAP) function [34] and decreased rRNA and tRNA synthesis, diverting resources away from unessential transcription and translation [29,35]. In addition, the stringent response inhibits cellular metabolism while simultaneously allowing redirection of resources previously utilized for this purpose to upregulate amino acid biosynthesis and production of universal stress proteins for stress defense [29]. While definitive answers about the details of (p)ppGpp targets and its mechanism of action remain controversial, progress has been made in gaining knowledge about and better understanding the complexities of its role in the stringent response pathway.

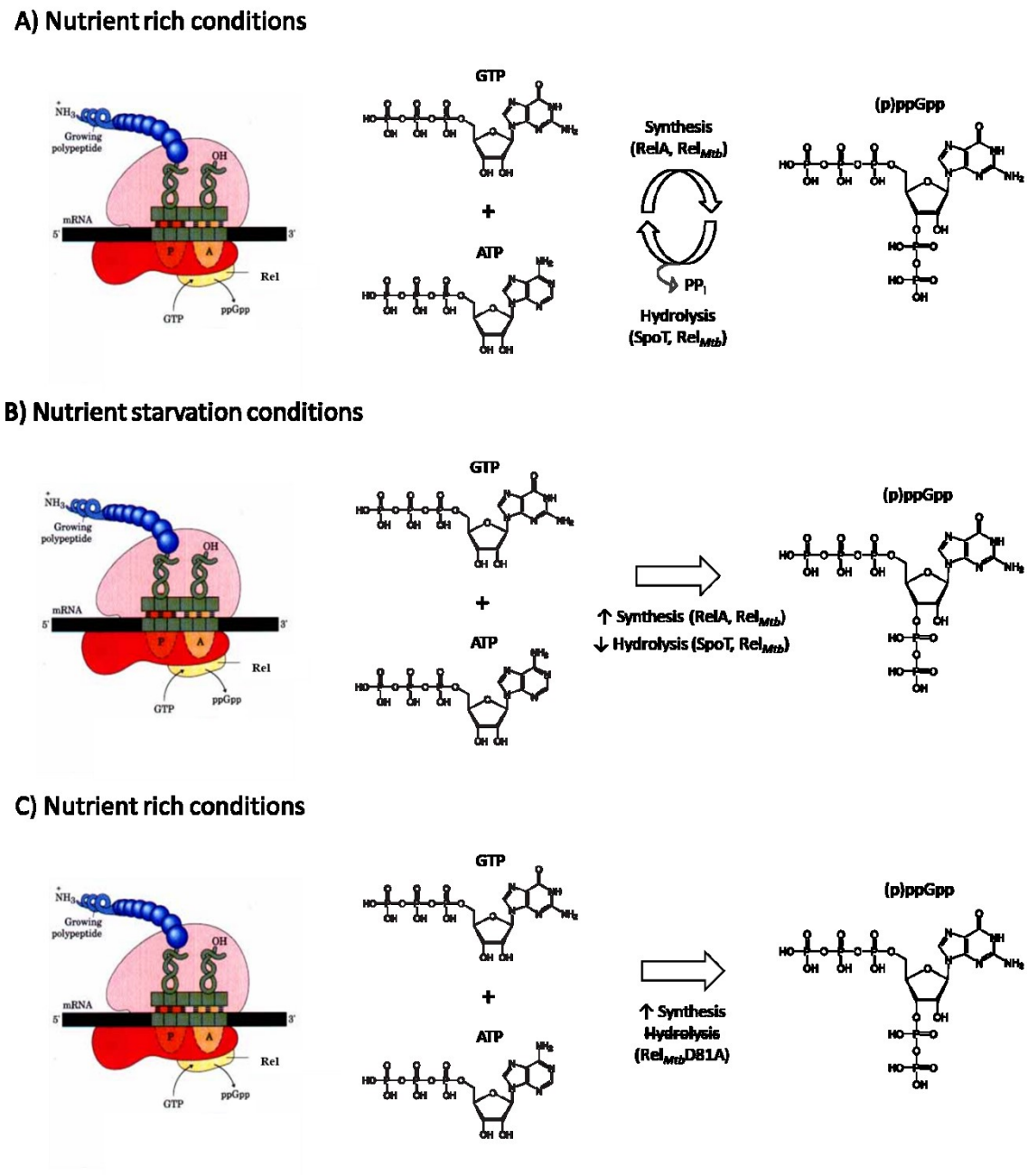

Figure 5 (p)ppGpp synthesis and hydrolysis in nutrient rich and nutrient starvation conditions (p)ppGpp is maintained at different levels depending on nutrient availability within the cell. Shown is the reaction for GTP and ATP. The reaction for GDP and ATP is the same, with the exception of beginning the reaction with GDP instead of GTP. A) In nutrient rich conditions monofunctional E. coli RelA or bifunctional *M. tuberculosis* Rel$_{Mtb}$ synthesizes baseline amounts of (p)ppGpp by removing two terminal phosphates from ATP to GTP, leaving AMP as a byproduct. E. coli SpoT or M. tuberculosis Rel$_{Mtb}$ hydrolyzes (p)ppGpp at baseline levels by removing the two 3' phosphates from (p)ppGpp, creating inorganic pyrophosphate (PP$_i$) as a byproduct, to maintain homeostatic amounts of (p)ppGpp. B) In nutrient starvation conditions RelA or Rel$_{Mtb}$ synthesis rates and affinity for GTP, GDP, and ATP increase, whereas SpoT or Rel$_{Mtb}$ affinity for (p)ppGpp and hydrolysis rates decrease. The resulting accumulation of (p)ppGpp induces the stringent response. C) Predicted accumulation of (p)ppGpp and induction of the stringent response in nutrient rich conditions under experimental conditions where hydrolysis-deficient Rel$_{Mtb}$ synthesizes (p)ppGpp without the accompanying hydrolysis necessary to maintain homeostatic levels of this alarmone.

At least one ppGpp binding site exists in *Escherichia coli* RNAP and transcriptional regulation after binding of the alarmone is evidenced by reduced synthesis of genes known to be under stringent control [36]. The crystal structure of ppGpp bound to *Thermus thermophilus* RNAP also suggests multiple possible mechanisms for this transcriptional regulation [34]. In addition, DnaK suppressor A (DksA), a protein connected to the cellular stress response [37] and required for rRNA regulation in changing environmental conditions [38], enhances ppGpp stability and transcriptional inhibition when both are bound to the *E. coli* RNAP. As determined by the crystal structure of DksA and biochemical analyses, a coiled coil is present at the tip of the protein which is located at the catalytic center of RNAP. Upon modeling of the *T. thermophilus* RNAP-ppGpp-DksA complex based on separate crystal structures of each molecule, one of two ppGpp bound magnesium ions (Mg^{2+}) at the catalytic center of the RNAP is likely coordinated by DksA. The bonds that form this coordination are thought to occur first, stabilizing ppGpp and allowing DksA to negotiate binding to the RNAP as it wraps around the structure with a hinge-like motion [39]. In addition to direct effects on RNAP, sigma factor binding is also altered in the stringent response, potentially facilitating broad transcriptional changes.

Working in concert with each other, the molecules involved in the stringent response pathway produce a persistent, nonreplicating physiological state. This altered state facilitates bacterial persistence and LTBI in the face of antibiotic and immune pressure, despite the lack of genetic resistance to many cell wall-active antibiotics [29]. The endurance of these bacteria culminates in increased bacterial survival and is thought to be one of several barriers to reducing the duration of treatment and curing disease in patients. Prompting phenotypically tolerant bacteria to emerge from dormancy by modulating the stringent response may render persistent, antibiotic tolerant pathogens more susceptible to killing by first-line antibiotics. A

particular target of interest central to this concept, RelA in *Escherichia coli* is a well-studied protein that remains a major component in regulating (p)ppGpp production and activation of the stringent response.

RelA and SpoT in *Escherichia coli*

Escherichia coli is a Gram-negative, rod shaped coliform found ubiquitously in the environment [9]. Both nonpathogenic and pathogenic strains of *E. coli* are prevalent, among which exist enterohemorrhagic serotypes associated with diseases such as food-borne illness and hemolytic uremic syndrome [40]. Despite more than fifty years of dedication to uncovering the intricacies involved in the stringent response, the roles of *E. coli* enzymes RelA and SpoT in this pathway remain complex and our understanding limited. Most studies of these enzymes occur under amino acid deprivation, but varying responses ensue under different stressors. Simply altering the type of nutrient withheld can eliminate or produce dramatic changes in numerous aspects of cellular physiology [29]. While there is still much to learn about the complexities of these enzymes, considerable progress has been made in elucidating their roles in the stringent response.

Under nutrient restriction, specifically amino acid deprivation, RelA operates as a monofunctional enzyme requiring Mg^{2+} to perform the (p)ppGpp synthesis described above [41,42]. SpoT is a bifunctional enzyme also capable of synthesizing (p)ppGpp under specific conditions. Its predominant function, however, is manganese (Mn^{2+}) dependent (p)ppGpp hydrolysis and degradation [43,44] to maintain homeostatic levels of this molecule. In addition to Mg^{2+}, (p)ppGpp synthesis by RelA also requires ribosomes, cognate mRNA, and uncharged tRNA positioned in the receptor site of the ribosomal complex [45]. RelA binds to this ribosomal complex at a unique location, both the 50s and 30s subunits interacting with the end of the RelA

C-terminus. The positioning of RelA in this manner allows the acceptor end of the uncharged A-site tRNA to bind and wrap around the beginning of the C-terminus, sterically hindering binding of charged tRNA, stalling protein synthesis, and presumably promoting (p)ppGpp synthesis by RelA [46].

The *Mycobacterium tuberculosis* enzyme Rel_{Mtb}

Unlike *E. coli* [29] and other organisms [25,42,47], *M. tuberculosis* encodes a bifunctional Rel/SpoT homolog (RSH) 738 amino acids in length with both phosphotransferase and phosphohydrolase activities. Rel_{Mtb} contains a C-terminal domain (CTD) and an N-terminal domain (NTD) [48] (Figure 6A). The NTD, which is responsible for dual synthesis and hydrolysis of (p)ppGpp [32] (Figure 5A), contains overlapping subdomains with separate catalytic sites for each of these two functions [49] (Figure 6B). The transferase activity of both RelA and Rel_{Mtb} depends upon the presence of Mg^{2+}. However, while providing these metal ions in excess does not limit monofunctional RelA performance [42], inhibition of bifunctional Rel_{Mtb} (p)ppGpp synthesis does occur due to a charge reversal in a conserved motif within the synthesis subdomain [42,49]. Additionally, the hydrolysis subdomain of Rel_{Mtb} relies on Mn^{2+} for hydrolysis function and, like its synthesis counterpart, is inhibited by excess levels of Mn^{2+} [49]. Furthermore, specific amino acid residues critical for transferase and hydrolase activity have been identified. Mutation of either the glycine or histidine at position 241 or 344, respectively, is sufficient to eliminate the synthesis function of the NTD while maintaining the ability to hydrolyze (p)ppGpp [48]. Conversely, an amino acid doublet in a conserved region of the hydrolysis subdomain is predicted to be essential for coordinating cations [50] and mutation of either the histidine or aspartic acid at position 80 or 81, respectively, abolishes hydrolysis activity while at the same time leaving synthesis function intact [48] (Figure 6B).

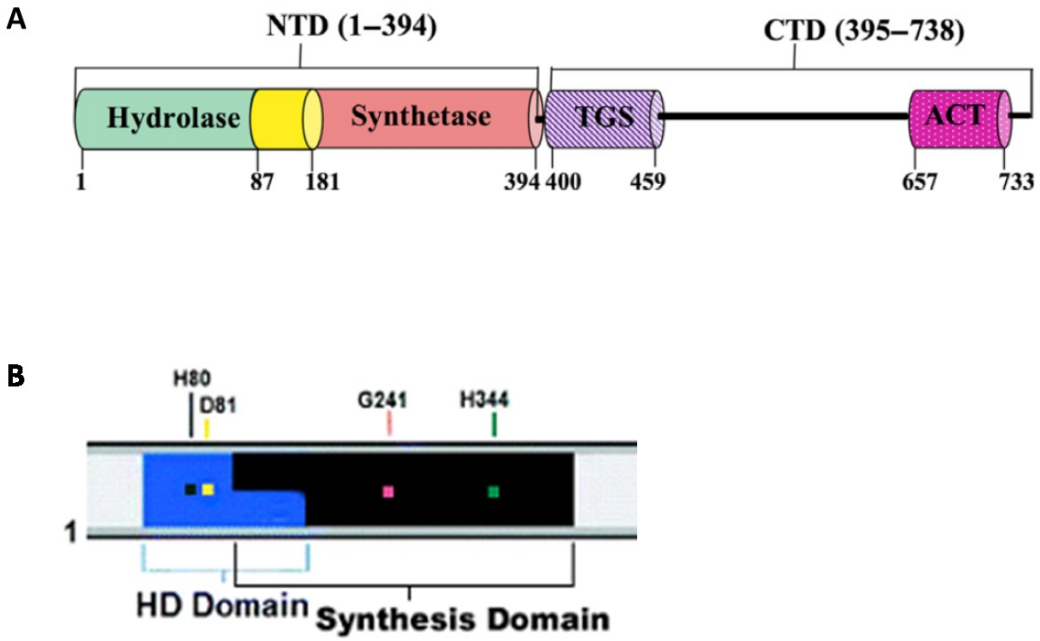

Figure 6 Schematic of mycobacterial Rel NTD and CTD Spatial representation of known subdomains of the full length mycobacterial Rel protein. A) NTD (1-394) containing the hydrolase (green), synthetase (salmon), and overlapping hydrolase/synthetase (yellow) subdomains. CTD (395 – 738) containing the TGS (purple) and ACT (pink) subdomains of the full length mycobacterial Rel protein [73]. B) Hydrolysis and synthesis subdomains of mycobacterial Rel with the HD domain (blue). Specific amino acid residues essential for hydrolysis or synthesis function are indicated by small colored squares [48].

While purified, full length Rel_{Mtb} is capable of simultaneous maximal (p)ppGpp synthesis and maximal hydrolysis [49], regulation of these NTD functions occurs at several levels in the presence of biological regulators and is often mediated by the CTD. The Rel_{Mtb} activating complex (RAC) is a combination of the Rel_{Mtb} enzyme, ribosomes, tRNA, and cognate mRNA. Utilizing this RAC, Rel_{Mtb} is capable of altering the rate of its synthesis and hydrolysis functions. When the RAC contains charged tRNA, representing abundant availability of nutrients, both the synthesis and hydrolysis functions remain at basal levels. However, in the presence of uncharged tRNA, representing amino acid depletion and mimicking starvation conditions, the synthetase affinity for its GTP/GDP/ATP substrates increases, as well as the rate of (p)ppGpp synthesis. Concurrently, the affinity of the hydrolase for its (p)ppGpp substrate and the rate at which it catalyzes hydrolysis is considerably reduced, leading to accumulation of (p)ppGpp and induction of the stringent response. In contrast, when the CTD is not present, the synthesis and

hydrolysis rates remain at basal levels even in the presence of the RAC. This lack of regulation in the absence of the CTD is consistent regardless of whether the NTD contains the synthetase, hydrolase, or both subdomains [48]. The mechanism of CTD regulation has been further studied in *Mycobacterium smegmatis*, a nonpathogenic species of *Mycobacteria* often used to inform future studies in *M. tuberculosis*.

M. smegmatis contains a bifunctional RSH termed Rel_{Msm} with a similar NTD comprised of phosphosynthetase and phosphohydrolase subdomains and a CTD containing a **T**hreonyl tRNA synthetase, **G**TPase, and **S**poT (TGS) subdomain, as well as an **A**spartate kinase, **C**horismite mutase, and **T**yrA (ACT) subdomain (Figure 6A). Rel_{Msm} (p)ppGpp synthesis increases in the presence of uncharged tRNA. However, when the CTD of Rel_{Msm} is cleaved, leaving only the NTD, the synthesis reaction is no longer affected by addition of uncharged tRNA [51]. Mutation of four cysteine residues conserved across RSH reveals mutation of the cysteine at position 692 is required to render full length Rel_{Msm} unresponsive to uncharged tRNA. Fluorescence resonance energy transfer and anisotropy measurements indicate a conformational change suggesting movement of the cysteine at position 692 away from the NTD into a more compact CTD formation when uncharged tRNA binds to Rel_{Msm}, providing more space for synthesis substrates to enter the catalytic site at the appropriate subdomain [52]. This finding is supported by the existence of a flexible, conserved linker region between the TGS and ACT subdomains [53]. In addition to regulation by an uncharged tRNA induced conformational change of the CTD, alternate ligand binding to this portion of Rel_{Msm} can cause the protein to unfold and decrease synthetase activity. Isothermal titration calorimetry confirms binding of (p)ppGpp to the Rel_{Msm} CTD at two separate regions that are potentially adjacent to each other when the protein's tertiary structure is intact. Though this (p)ppGpp binding is weak, mutations at conserved residues within the two identified regions abolish the ability of excess (p)ppGpp to decrease

synthesis, leading to the idea of a negative feedback loop between Rel_{Msm} and (p)ppGpp that regulates (p)ppGpp accumulation within the bacteria [54].

In addition to regulation at the enzymatic level, components in the cell also regulate Rel_{Mtb} transcription. Among other functions, the transcription factor Sigma factor E (SigE) aids in increasing transcription of Rel_{Mtb} [55]. In the *mprAB-sigE-rel* pathway inorganic polyphosphate [poly(P)] chains are utilized to phosphorylate MprB, the first unit of a two-component signal transduction system. In the second step of this system MprB phosphorylates MprA, consequently inducing synthesis of SigE and increased transcription of Rel_{Mtb}. Upstream of this signaling pathway, polyphosphate kinase (PPK) synthesizes poly(P) from ATP and inorganic phosphate (P_i) stores in the cell. Two hydrolytic exopolyphosphate kinases, PPX1 and PPX2, in turn degrade poly(P), maintaining a balance of the molecule in the cell. Increasing levels of poly(P) also induce the stringent response, assisting in survival during the stress conditions of stationary phase culture [57]. (p)ppGpp inhibition of PPX hydrolysis is postulated to allow the buildup of poly(P) chains in the cell, which feed into the *mprAB-sigE-rel* signaling pathway by preferentially phosphorylating MprB and consequently increasing Rel_{Mtb} transcription as described above.

Rel_{Mtb} not only produces (p)ppGpp in cell-free systems, but also during nutrient starvation in its native *M. tuberculosis*. A Rel_{Mtb} knockout strain (Δrel_{Mtb}) does not produce (p)ppGpp at detectable levels and displays a survival defect in various nutrient depleted systems [28]. *In vivo* results in mice [58] and guinea pigs [59], both model organisms for persistent TB infection, mirror the *in vitro* phenotype of reduced survival. While the bacterial burden in lung tissue remains the same for wild type and Δrel_{Mtb} strains in the acute phase of infection, the bacterial burden in lungs of animals exposed to Δrel_{Mtb} is reduced during the chronic phase of infection [58,59]. In addition, gross pathology and histopathology of lung tissues are less severe

in *Δrel*$_{Mtb}$-infected animals [58]. This attenuated phenotype of the *Δrel*$_{Mtb}$ strain, particularly during the chronic phase of infection, and association of the knockout with altered expression of genes important for survival under stress, establishes Rel$_{Mtb}$ as an important factor in long-term survival of *M. tuberculosis* in the host. However, much remains to be understood about this multifaceted regulator of the stringent response. Additional studies are necessary to investigate questions that persist and illuminate mechanistic details.

Study outline

The attenuated phenotype of *Δrel*$_{Mtb}$ suggests the stringent response pathway may represent a significant therapeutic target. Disrupting the stringent response through modulation of Rel$_{Mtb}$ provides the opportunity to gain a better understanding of this pathway in mycobacterial persistence. Therefore, a complementary approach to the currently published Rel$_{Mtb}$ knockout studies is proposed and creation of a strain capable of inducible Rel$_{Mtb}$ overexpression and (p)ppGpp accumulation has been undertaken. Specifically, this thesis details generation of a *rel*$_{Mtb}$ knock-in strain using molecular cloning techniques. Previous studies have shown that (p)ppGpp hydrolysis function is eliminated in a recombinant Rel$_{Mtb}$ protein containing a point mutation leading to an amino acid change at codon 81 in the hydrolysis domain, while (p)ppGpp synthetic function is not affected [48]. Site-directed mutagenesis was employed to create this point mutation, modifying the aspartic acid at position 81 to an alanine. The hydrolysis-deficient *rel*$_{Mtb}$ gene was cloned into a tetracycline-inducible *M. tuberculosis* plasmid containing a hygromycin resistance cassette. After confirmation of successful gene insertion by gel electrophoresis and Sanger sequencing, the plasmid was transformed into the wild type *M. smegmatis* laboratory strain mc^{2}155. Upon selection of successfully transformed hygromycin resistant colonies, inducible expression of *rel*$_{Mtb}$ was confirmed at both the gene and

protein level by quantitative polymerase chain reaction (qPCR) and western blot, respectively. Consequently, this hydrolysis-deficient *rel*$_{Mtb}$ knock-in strain of *M. smegmatis* can be used to characterize mycobacterial phenotypes during induction of the stringent response. In addition, while the tet$_{on}$ knock-in system described here is capable of answering relevant *in vitro* questions, it is also a tool that can be easily extended to future *in vivo* experiments due to the bioavailability and tolerability of the inducing agent, doxycycline.

Utilizing a *rel*$_{Mtb}$ knock-in strain that permits inducible accumulation of (p)ppGpp allows validation of the hypothesis that induction of the stringent response is sufficient for entry into a growth restricted, persistent state. Understanding the role of Rel$_{Mtb}$ and learning how to modulate the stringent response in the laboratory introduces the possibility of targeting persistent bacilli using small molecule inhibitors of the Rel$_{Mtb}$ enzyme. Using this strategy, bacteria may be rendered susceptible to killing by cell wall-active agents targeting replicating organisms. This novel therapeutic approach may allow current antibiotics to work more efficiently and, therefore, shorten the duration of curative treatment for TB.

Materials and Methods

Culture conditions and plasmid isolation

All *Escherichia coli* cultures were grown in Luria-Bertani (LB) broth (VWR J106-500G) or on LB agar containing 200µg/mL hygromycin (Sigma H3274-100MG) or 100µg/mL ampicillin (Sigma A9518-5G) for 16 – 20 hours. Plasmids were isolated from culture using the QIAprep spin miniprep kit (Qiagen 27104) following the manufacturer's protocol. *M. smegmatis* mc^{2}155 cultures were grown in Middlebrook 7H9 broth (Becton Dickinson 271310) supplemented with 0.4% glycerol (Fisher Scientific G33-500), 10% OADC (Becton Dickinson 212351) and 0.05% Tween 80 (Fisher Scientific BP338-500) until log phase (0.1-0.6 OD) or on 7H10 agar (Becton

Dickinson 262710) supplemented with 1% glycerol and 10% OADC for four days unless stated otherwise.

PCR amplification for molecular cloning

Genes of interest were amplified from specified genomic DNA sources using the polymerase chain reaction (PCR) with Platinum Hot Start PCR 2x Master Mix (Invitrogen 13000-012). PCR reactions were carried out according to the manufacturer's protocol. Briefly, components were mixed to achieve the following final concentrations: 1x Platinum Master Mix, 20% Platinum GC Enhancer, 0.2µM forward and reverse primers (Table 1), ~100ng template DNA, and nuclease free water to 25µL. Reactions were performed on a Bio-Rad MyCycler thermal cycler at an initial denaturation temperature of 94°C for 2 minutes followed by thirty-five cycles of denaturation at 94°C for 30 seconds, annealing at temperature corresponding to specific primers listed in Table 1 for 30s, and extension at 72°C for 1 minute/kb (2 minutes for rel_{Mtb} and 1 minute for *gfp*). Reactions were then held at 4°C until used for molecular cloning.

Agarose gel electrophoresis

All PCR and plasmid amplifications, as well as restriction digests, were confirmed by agarose gel electrophoresis. Briefly, the entire volume of plasmid product or a 5µL aliquot of gene product was mixed with 6x loading dye (NEB B7024S or Fisher Scientific R0611) to a final concentration of 1x loading dye. Samples were loaded into an agarose gel containing final concentrations of 1x Tri-acetate-EDTA (TAE), 1% agarose (BioWhittaker Molecular Applications 5004), 0.5µg/mL ethidium bromide (Sigma E1510-10mL), and DI water to the desired final volume. A GeneRuler 1kb Plus DNA ladder (Fisher Scientific SM0314) was loaded as a known standard to compare and identify sizes of DNA products and gels were run at 80V for 45

minutes. Gels were imaged using a Bio-Rad Gel Doc EZ imager or, alternatively, a Spectroline ultra violet transilluminator when DNA excision was required.

Molecular cloning

Genes of interest were PCR-amplified as detailed above. PCR products were purified using the QIAquick PCR purification kit (Qiagen 28104) according to the manufacturer's protocol, followed by digestion with the indicated restriction enzymes (RE, Table 2). Plasmids of interest were digested concurrently using RE listed in Table 2. Briefly, 200ng PCR products or 1µg isolated plasmid were combined with restriction digest buffer and RE for final concentrations of 1x CutSmart buffer (NEB B7204S) and 10 units of each appropriate RE (Table 2). Nuclease free water was used to achieve a final volume of 20µL where necessary, and the digestion carried out at 37°C for 2 hours. After digestion, 1µL of calf intestinal phosphatase (CIP, NEB M0508S) per 3kb DNA was added to each reaction in order to prevent DNA ends from ligating to each other. Reactions were incubated at 37°C for an additional 10 minutes, followed by deactivation of CIP at 80°C for 2 minutes and holding at 4°C. Digestion was confirmed by agarose gel electrophoresis as described above and the desired plasmid fragments were excised and purified using the QIAquick gel extraction kit (Qiagen 28704) according to the manufacturer's protocol. Digested PCR products were also purified using the QIAquick PCR purification kit. Digested plasmid and PCR products were combined in a 1:3 molar ratio (plasmid:gene) with addition of T4 DNA ligase (NEB M0202S) and ligation buffer (NEB B0202S) at final concentrations of 5% T4 DNA ligase and 1x buffer. Nuclease-free water was added to bring the final volume to 20µL when necessary and ligation commenced at room temperature for 30 minutes.

Transformation by heat shock

Ligation products were transformed into MAX efficiency DH5α competent *E. coli* cells (Invitrogen 18258012) using the heat shock method according to the manufacturer's protocol. Briefly, 1µL of ligation products was added to 50µL of competent cells and incubated at room temperature for 1 hour. The mixture was heat-shocked for 90 seconds at 42°C using a BioExpress GeneMate digital dry bath heat block to permeabilize bacteria and subsequently cooled on ice for 2 minutes. Super optimal broth with catabolite repression (SOC broth, NEB B9020S) was added to cells in a 1:10 ratio (cells:broth) and incubated with shaking for 1 hour at 37°C to allow expression of antibiotic resistance genes. The entire volume of each culture was plated on separate LB agar plates containing antibiotics according to the resistance cassette present in the transformed plasmid and plates were incubated at 37°C for 16 hours. Resulting colonies were selected for regrowth in antibiotic-containing LB broth and screened for the inserted gene of interest by a modified form of colony PCR, as described below. Individual colonies positive by PCR were subcultured in 11mL of LB broth containing appropriate antibiotics and incubated at 37°C for 20 hours. Culture stocks containing 50% glycerol were stored at -80°C. Plasmid was isolated from the remaining culture, as described above, in order to confirm gene insertion by Sanger sequencing, as detailed below, and for use in future experiments.

Site-directed mutagenesis

In preparation for site-directed mutagenesis (SDM) of rel_{Mtb}, the gene was PCR-amplified from the H37RvSA laboratory strain of *M. tuberculosis* [28] using rel_{Mtb} primer sequences listed in Avarbock et al [32] (Table 1) and cloned into a pET15b plasmid vector, as detailed above. SDM was performed using the QuikChange Lightning Site-Directed Mutagenesis kit (Agilent

Technologies 210518) with minor changes to the manufacturer's protocol. Briefly, complementary mutagenic PCR primers were designed to include a single nucleotide difference yielding an amino acid change from aspartic acid to alanine at codon 81 of the *rel*$_{Mtb}$ gene (Table 1). The mutant plasmid was synthesized by PCR using these primers and the non-mutated parental plasmid DNA was digested using a DpnI RE to improve transformation efficiency of the mutated plasmid. Due to both the cells provided in the QuikChange Lightning SDM kit and the pET15b plasmid containing an ampicillin resistance cassette, alternative cells were required to screen for plasmid-containing cells by antibiotic resistance. Therefore, 2µL of mutated plasmid was transformed into MAX efficiency DH5α competent *E. coli* cells using the heat shock method, as described above. Individual colonies were screened for *rel*$_{Mtb}$ by colony PCR and stocks were made, as detailed above. Plasmid DNA was isolated from PCR-positive cultures and the correct point mutation confirmed by Sanger sequencing, as described below. This plasmid was designated pET15b/Rel$_{Mtb}$D81A

Rel$_{Mtb}$D81A and GFP control plasmid construction

gfp and *rel*$_{Mtb}$D81A were PCR-amplified from pUV15tetORm and pET15b/Rel$_{Mtb}$D81A (Table 1), respectively, and cloned into both the pUV15tetORm_F plasmid and the pUV15tetORm_R plasmid (Table 2), as described above. Newly ligated plasmids were transformed into *E. coli* by the heat-shock method and colonies were selected on LB plates containing 200µg/mL hygromycin, as detailed above. Gene insertion was confirmed by colony PCR and Sanger sequencing, as described below, to yield three plasmids: pUV15tetORm_FGFP, pUV15tetORm_RGFP, and pUV15tetORm_FRel$_{Mtb}$D81A plasmids.

Colony PCR for preliminary confirmation of gene insertion

The modified form of colony PCR described here was used to screen transformants for the gene of interest before sending samples for definitive confirmation by Sanger sequencing, detailed in a separate section below. Genes of interest were PCR-amplified from culture with *Taq* DNA Polymerase (NEB M0267S) according to the manufacturer's protocol. Briefly, components were mixed to achieve the following final concentrations: 1.25U *Taq* DNA Polymerase, 1x ThermoPol reaction buffer, 200µM dNTPs (Thermo Scientific R0192), 0.2µM forward and reverse primers (Table 1), 1µL culture, and nuclease-free water to a total volume of 25µL. Reactions were performed on a Bio-Rad MyCycler thermal cycler at an initial denaturation temperature of 95°C for 30 seconds followed by thirty-five cycles of denaturation at 95°C for 30 seconds, primer-specific annealing at temperatures listed in Table 1 for 1 minute, and extension at 68°C for 1 minute/kb (2 minutes for rel_{Mtb} and 1 minute for *gfp*). A final extension was performed at 68°C for 5 minutes and reactions were then held at 4°C until confirmation of PCR amplification by agarose gel electrophoresis, as described above.

Sanger sequencing

This section details sample preparation for Sanger sequencing completed by Eurofins Genomics LLC, and confirmation of sequence similarity to the appropriate publicly available DNA sequence by BLAST analysis. The plasmid of interest was combined with a single desired primer (Table 3) for final concentrations of 66.7ng/µL plasmid and 0.2µM primer in a 12µL volume. Samples were labeled and sent to Eurofins Genomics for Sanger sequencing in accordance with the company's protocols. BLAST analysis was performed by aligning plasmid sequencing reads with appropriate known DNA sequences. Reads having ≥90% similarity to their respective known sequence were considered confirmed as matching the DNA sequence in question.

Transformation by electroporation

The pUV15tetORm_FGFP, pUV15tetORm_RGFP, and pUV15tetORm_FRel$_{Mtb}$D81A plasmids were isolated from *E. coli* cultures and transformed into wild type *M. smegmatis* by electroporation as described by Larsen [60]. Briefly, *M. smegmatis* was grown to mid-log phase (OD 0.5), incubated for 10 minutes on ice, pelleted by centrifugation, and washed with one volume of ice-cold 10% glycerol three times before final resuspension in 10% glycerol at 1/10th the original culture volume. 400µL of *M. smegmatis* culture and 2µL of plasmid were mixed on ice in a pre-chilled Gene Pulser cuvette with a 0.2cm electrode gap (BioRad 165-2082) and electroporated using a Bio-Rad GenePulser II set at 2.5kV, resistance 1,000Ω, and capacitance 25µF. 2mL of media was added immediately after transformation and cultures were incubated with shaking for 2 hours at 37°C to allow expression of antibiotic resistance genes, followed by plating 50µL of culture on 7H10 agar containing 50µg/mL hygromycin. Plates were incubated at 37°C and colonies selected after four days of growth. Integration of the respective gene of interest was confirmed by PCR amplification, as described above, after DNA isolation, as detailed below, as well as Sanger sequencing.

DNA isolation

M. smegmatis genomic DNA was isolated either by scraping a single colony from agar or pelleting 10mL of culture, resuspending in 600µL of media, and transferring to a 2mL lysing matrix B tube containing 0.1mm silica beads (MP Biomedicals 6911-050). Regardless of the source, an equal volume of phenol solution (Sigma P4557-400ML) was added and bacteria vortexed for 1 minute at maximum speed. Samples were then centrifuged for 2 minutes at 16,000g, the top layer transferred to one volume of chloroform/isoamyl (24:1)[choloform (Fisher Scientific C289-500):isoamyl (J.T.Baker 9038-01)], vortexed briefly, and centrifuged for 2

minutes at 16,000g. The aqueous layer was transferred to 1/10th volume of 3M sodium acetate (Fisher Scientific 5210-500) with subsequent addition of two volumes of 100% EtOH. Samples were pelleted by centrifugation for 15 minutes at 16,000g, followed by two washes with 70% ethanol and air-dried for 15 minutes. DNA was resuspended in 100µL Tris-EDTA (TE) buffer, the concentration determined by measurement using a NanoDrop 2000 spectrophotometer, and stored at -20°C.

RNA isolation and qRT-PCR

In preparation for RNA isolation a 10mL culture of *M. smegmatis* was pelleted, resuspended in 1mL of TRIzol (Ambion 15596018), and subjected to bead beating in 2mL lysing matrix B tubes containing 0.1mm silica beads (MP Biomedicals 6911-050) using a Bead Bug Microtube Homogenizer at speed 400x10 for 1 minute. 200µL of chloroform was added to each sample and centrifuged for 10 minutes at 20,000g and 4°C. The aqueous phase was removed into an equal volume of 70% ethanol and RNA was isolated following the manufacturer's protocol for the RNeasy mini kit (Qiagen 74104). RNA was eluted in 30µL of EB buffer and concentrations were determined by Nanodrop measurement and stored at -20°C. cDNA was synthesized from isolated RNA using the QuantiTect reverse transcription kit (Qiagen 205314) and following the manufacture's protocol with the exception of adding RNase free water for a final volume of 70µL and a final concentration of 0.63ng/µL cDNA. qPCR was performed utilizing the QuantiTect SYBR Green PCR kit (Qiagen 204143) and halving the volumes used in the manufacturer's protocol. Analysis was performed using the $2^{-\Delta\Delta CT}$ method. qPCR primers for *mysA*, *gfp* and rel_{Mtb} were designed as indicated in Table 1 and 5µL of cDNA was used for each reaction.

Protein collection and western blotting

M. smegmatis protein was collected by pelleting 10mL of culture and resuspending in 300µL of protein buffer consisting of the following components at final concentrations of 1x RIPA buffer (Cell Signaling 9806S), 1x phosphatase inhibitor (Thermo Scientific 78428), and 1x protease inhibitor (Thermo Scientific 78430). Samples were subjected to bead beating as described for RNA isolation and qRT-PCR and supernatant transferred to new microcentrifuge tubes. A colorimetric BCA protein assay (Pierce 23227) was performed to quantify the amount of total protein in each sample and determine the volume of protein utilized for western blotting. 20µg of total protein was run on a 4%-15% Mini PROTEAN TGX gel (BioRad 456-1086) using a SeeBlue Plus2 prestained standard (Invitrogen LC5925) as a known standard to compare and identify approximate sizes of protein bands. Gels were run at 150V for 1 hour and transferred to a nitrocellulose membrane (BioRad 162-0097) using a BioRad Trans-Blot SD Semi-Dry transfer cell set at 20V for 25 minutes. The membrane was washed in TBST (1x TBS (BioRad 1706435) and 0.1% Tween 20 (Sigma P1379-100ML)) for 5 minutes at room temperature and all subsequent washes conducted in the same manner. The membrane was then incubated in blocking buffer (5% nonfat dry milk (BioRad 170-6404), 1xTBS, 0.05% Tween 20) for 1 hour, washed three times, and incubated covered overnight at 4°C with a Rel_{Mtb} primary antibody from mouse serum. The membrane was then washed three times and incubated for 45 minutes with an HRP secondary antibody (Thermo Fisher A16166). Following four washes the membrane was exposed to a chemiluminescent substrate (Pierce 32109) and protein bands viewed by chemiluminescence, exposing the membrane to film (Thermo Scientific 34090) for 5 minutes immediately after introducing the chemiluminescent substrate and developing on a AFP Mini-Medical Series developer.

Anhydrotetracycline induction time course

Large volumes of pUV15tetORm_FGFP and pUV15tetORm_FRel$_{Mtb}$D81A culture were grown to an OD of 0.1, whereupon anhydrotetracycline (aTC, 100ng/mL [61]) was added and this day designated as day 0. Samples were collected for RNA isolation with time points every four hours during the first twenty-four hour period and additional time points at 36 hours, 44 hours, 48 hours, and 72 hours. RNA was isolated and qRT-PCR performed, as stated above, to assess expression levels of the gene of interest at specified time points during growth.

Growth kinetics assay

Large volumes of pUV15tetORm_FGFP and pUV15tetORm_FRel$_{Mtb}$D81A culture were grown to an OD of 0.1, whereupon anhydrotetracycline (aTC, 100ng/mL) was added and this day designated as day 0. OD was measured every four hours for the first twenty-four hour period with additional measurements at 36 hours, 44 hours, 48 hours, and 72 hours. OD values were graphed with respect to time to assess growth kinetics of each bacterial strain.

Results

Isolation of *rel$_{Mtb}$* and *rel$_{Mtb}$*H80A

A balance between the (p)ppGpp synthesis and hydrolysis activities of Rel$_{Mtb}$ is required for normal homeostatic functioning of *M. tuberculosis* (Figure 5A). Avarbock et al [48] has shown that specific point mutations eliminate the (p)ppGpp hydrolysis function of Rel$_{Mtb}$ while preserving the synthesis function of the enzyme. We hypothesize that overexpression of a hydrolysis-deficient version of Rel$_{Mtb}$ in *M. tuberculosis* would phenocopy induction of the stringent response, in which (p)ppGpp accumulates (Figure 5C).

A pET15b plasmid containing the wild type rel_{Mtb} gene from *M. tuberculosis* clinical strain CSU11/22 and a pET22b plasmid containing rel_{Mtb} from the same background with a hydrolysis ablating point mutation at amino acid 80 (rel_{Mtb}H80A; both kind gifts of Dr. Harvey Rubin, University of Pennsylvania) were individually transformed into *E. coli*. Although liquid cultures of *E. coli* containing the pET15b/Rel_{Mtb} plasmid achieved turbidity within 4 hours, those containing the pET22b/Rel_{Mtb}H80A plasmid did not become turbid until after three days. In order to confirm the presence of the desired plasmids, a diagnostic digest was performed on the pET15b/Rel_{Mtb} and pET22b/Rel_{Mtb}H80A plasmids using the respective enzymes listed in Table 2 and visualized by agarose gel electrophoresis. Expected DNA bands at sizes of 2214bp and 5406bp were visible for digested pET15b/Rel_{Mtb} (Figure 7), preliminarily confirming the presence of this plasmid and the gene of interest it contained. However, DNA bands were absent for

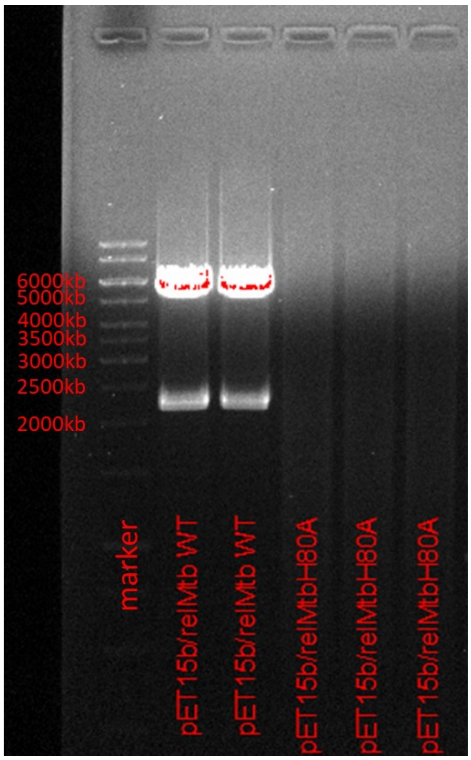

		Size of Gene Products (kb)	
		Nde1/BamH1 digest	Nde1/HindIII digest
Plasmid	pET15b/rel_{Mtb}WT		2214 5406
	pET22b/rel_{Mtb}H80A	2214 5403	

Figure 7 Diagnostic digest of pET15b/Rel_{Mtb} and pET22b/Rel_{Mtb}H80A Diagnostic digest of pET15b plasmids containing wild type Rel_{Mtb} (pET15b/Rel_{Mtb} WT, lanes 3 and 4) or hydrolysis-deficient Rel_{Mtb} (pET15b/Rel_{Mtb}H80A, lanes 5-7) conferred by a point mutation at position 80. The table indicates expected sizes of bands based on plasmid size and restriction enzymes utilized.

digested pET22b/Rel$_{Mtb}$H80A (Figure 7) despite quantification of nucleic acids by Nanodrop. As an alternative approach, larger volumes of pET22b/Rel$_{Mtb}$H80A culture were grown to obtain high enough plasmid concentrations for sequencing. With an adequate amount of plasmid available, samples were prepared and sent for sequencing of *rel*$_{Mtb}$ from both pET15b/Rel$_{Mtb}$ and pET22b/Rel$_{Mtb}$H80A plasmids using the primers listed in Table 3. Resulting reads were compared to the genetic sequence of *rel*$_{Mtb}$ obtained from Tuberculist [62] using BLAST analysis, and successfully confirmed the pET15b/Rel$_{Mtb}$ plasmid did indeed contain actual *rel*$_{Mtb}$. However, upon comparison of reads from pET22b/Rel$_{Mtb}$H80A with the genetic sequence of *rel*$_{Mtb}$ from Tuberculist in the same manner, no significant matches were observed. In a final effort to enhance production and confirm the presence of the pET22b/Rel$_{Mtb}$H80A plasmid, isolated plasmid was transformed into a new strain of DH5α *E. coli* by the heat shock method. No detectable transformants were visualized on LB/ampicillin plates despite successful transformation of a pUC19 control. Negative results obtained by diagnostic digest, Sanger sequencing, and transformation determined that further work with this sample would be abandoned in favor of synthesis of a new hydrolysis-deficient *rel*$_{Mtb}$ from *M. tuberculosis* genomic DNA.

Synthesis of hydrolysis-deficient Rel$_{Mtb}$D81A

Although the pET15b/Rel$_{Mtb}$ plasmid contained wild type *rel*$_{Mtb}$, the source of this gene was a clinical *M. tuberculosis* isolate. To ensure consistency with previously published studies and the majority of TB literature, *rel*$_{Mtb}$ was PCR-amplified from the well-characterized *M. tuberculosis* laboratory reference strain H37RvSA using the primers listed in Table 1, cloned into pET15b with the RE listed in Table 2, and the insertion was confirmed by Sanger sequencing using the primers listed in Table 3 followed by BLAST analysis against the Tuberculist *rel*$_{Mtb}$

genetic sequence. Mutation of amino acids at codon 80 or 81 abolishes Rel$_{Mtb}$ hydrolysis activity [48]. However, codon 81 requires only a single nucleotide change, whereas codon 80 requires two nucleotide changes. Therefore, a point mutation introduced by site-directed mutagenesis and yielding an amino acid change from aspartic acid to alanine at codon 81 of the *rel*$_{Mtb}$ gene was chosen to eliminate its hydrolysis function. This single nucleotide change was confirmed by Sanger sequencing using the primers listed in Table 3 followed by BLAST analysis against the Tuberculist *rel*$_{Mtb}$ genetic sequence (Figure 8) and the plasmid designated as pET15b/Rel$_{Mtb}$D81A.

Figure 8 Confirmation of *rel*$_{Mtb}$D81A site-directed mutagenesis by Sanger sequencing Results of BLAST analysis querying the wild type *rel*$_{Mtb}$ gene sequence against Sanger sequencing results of putative *rel*$_{Mtb}$D81A. The single nucleotide point mutation changing aspartic acid at position 81 to alanine and ablating hydrolysis function is boxed in red.

Confirmation of pUV15tetORm plasmid backbones and gene insertion

Overexpression of hydrolysis-deficient Rel_{Mtb}D81A is predicted to be sufficient to induce the stringent response through dysregulated accumulation of (p)ppGpp, resulting in slowed bacterial replication, even in nutrient rich conditions. However, we considered the possibility that excessively elevated (p)ppGpp levels due to constitutive overexpression of Rel_{Mtb}D81A may be lethal. Therefore, we pursued a strategy of conditional overexpression of Rel_{Mtb}D81A using a tetracycline-inducible system. A tetracycline controlled transactivator (tTA), created by fusion of a tetracycline repressor (tetR) and a virion protein from herpes simplex virus, binds to a repeat sequence of tetracycline operators (tetO) known as the tetracycline response element (TRE). This TRE is positioned upstream of a minimal promoter and binding of the tTA triggers expression of the gene of interest. In this tetracycline off (tet_{off}) system introduction of tetracycline reduces gene expression dramatically by binding to and removing tTA from the TRE [63]. However, reducing gene expression after addition of tetracycline in the tet_{off} system requires more than two days, posing the risk of stringent response induction at the initial phase of growth in the current study. In contrast, the tetracycline on (tet_{on}) system [64] possesses a mutated tTA that only binds to the TRE in the presence of tetracycline. Utilizing this system provides the opportunity for bacterial growth to log phase before inducing expression of Rel_{Mtb}D81A.

Another consideration was the ability to stably integrate the gene of interest into a mycobacterial genome. Inclusion of the *attP* attachment site and integrase originally found in the L5 mycobacteriophage has been shown to allow integration of plasmids that contain these elements into *M. smegmatis*, bacille Calmette-Guerin (BCG), and *M. tuberculosis* genomes [65]. Both the *attP* site in the plasmid and an *attB* attachment site in the bacterial genome possess a homologous core region that allows for site-specific recombination with assistance from the

integrase. The result is stable insertion of the plasmid sequence, including the gene of interest, into the bacterial genome at the *attB* site. Incorporating the gene of interest into the mycobacterial genome eliminates the need for continual antibiotic selection. It also provides the added advantage of enabling further study of any observed *in vitro* phenotypes in animal models due to stable maintenance of the gene of interest within the mycobacterial genome and the ability to use the well tolerated tetracycline analog doxycycline to induce expression of the gene of interest.

The tet_{on} plasmid pUV15tetORm containing a mycobacterial specific promoter, a gift from Sabine Ehrt (Addgene plasmid #17975) [66], was modified by previous lab member Dr. Yu-Min Chuang to include an *attP* attachment site and an integrase [56]. This plasmid backbone was designated as pUV15tetORm_F (Figure 9). *In vivo* experiments previously performed with a strain of *M. tuberculosis* containing the pUV15tetORm_F plasmid backbone integrated into its genome showed both the empty vector control lacking an inserted gene of interest and the test plasmid containing the gene of interest displayed a similar altered phenotype when compared to wild type *M. tuberculosis*. In order to determine whether the observed phenotype was an original phenomenon of the gene of interest or merely an effect of the plasmid backbone, the TRE and promoter were repositioned in the plasmid backbone to allow positioning of the gene of interest in a reverse orientation compared to the pUV15tetORm_F plasmid. This plasmid possessing the gene of interest in a reverse orientation was designated pUV15tetORm_R (Figure 9) and it was determined that the corresponding empty vector control did not display the altered phenotype seen previously. The observed phenotype was, therefore, attributed to the gene of interest and not a general effect of the plasmid backbone.

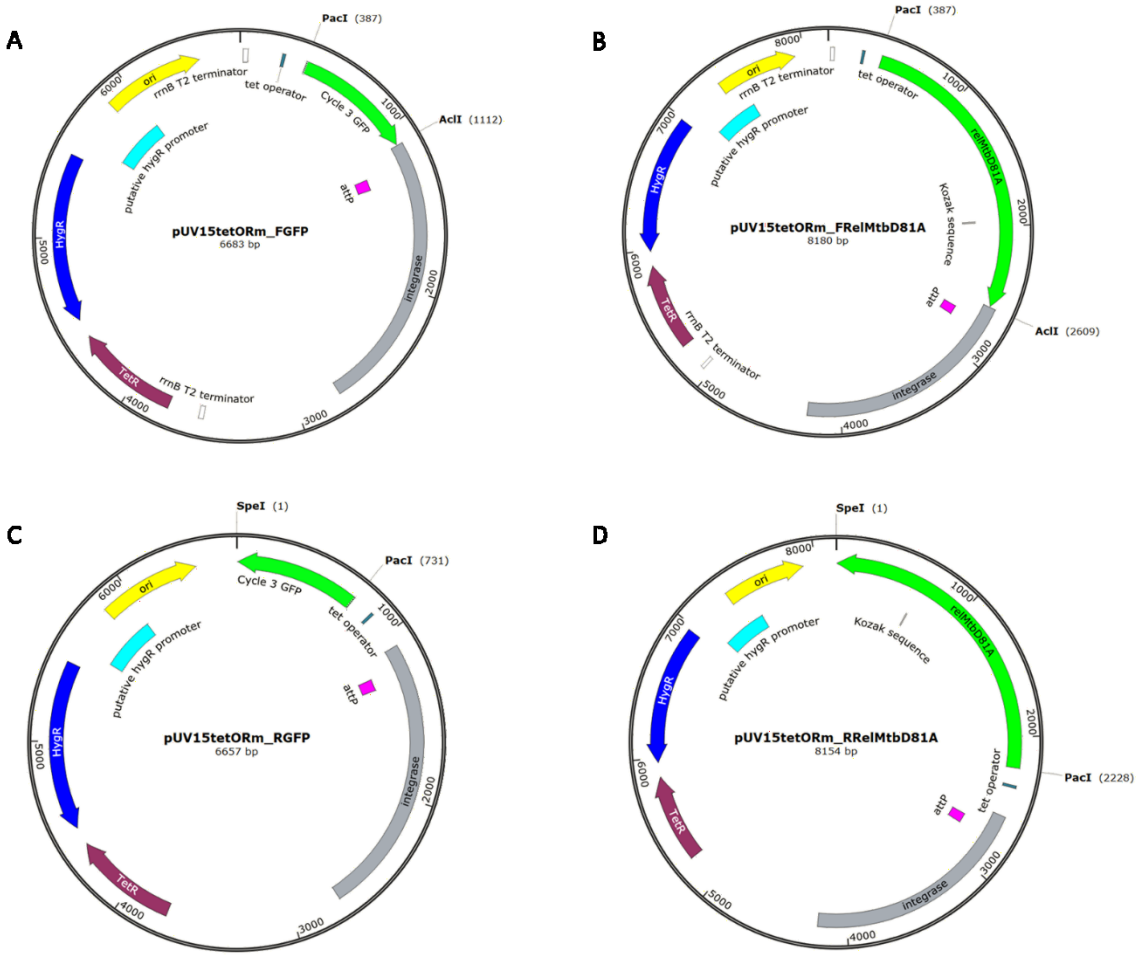

Figure 9 pUV15tetORm_F and pUV15tetORm_R plasmid maps Plasmid maps for pUV15tetORm_FGFP (A), pUV15tetORm_FRel$_{Mtb}$D81A (B), pUV15tetORm_RGFP (C), and pUV15tetORm_FRel$_{Mtb}$D81A (D) with relevant restriction enzymes and features displayed. Origin of replication (yellow), tetracycline operator (teal), gene of interest (green), attP site (pink), integrase (gray), tetracycline repressor (TetR, maroon), and hygromycin resistance cassette (dark blue).

Upon receipt of the pUV15tetORm_F and pUV15tetORm_R plasmids for the current study their identity was confirmed by diagnostic digest. This diagnostic digest was performed on the pUV15tetORm_F and pUV15tetORm_R plasmids using the respective enzymes listed in Table 2 and visualized by agarose gel electrophoresis. Two DNA bands at the expected sizes of 1000bp and 5968bp for digestion with AclI and PacI RE or 387bp and 6552bp for digestion with SpeI and PacI RE were visible after digestion of pUV15tetORm_F (Figure 10), preliminarily confirming its identity. Three DNA bands at the expected sizes of 351bp, 977bp, and 5602bp for digestion with AclI and PacI RE or two DNA bands at the expected sizes of 1000bp and 5926bp for digestion

with SpeI and PacI RE were visible after digestion of pUV15tetORm_R (Figure 10), also preliminarily confirming its identity. Additionally, Sanger sequencing using the primers listed in Table 3 followed by BLAST analysis against genetic sequences provided by Dr. Yu-Min Chuang also confirmed the identity of the two plasmid backbones. A majority of both the pUV15tetORm_F and pUV15tetORm_R plasmid reads were accounted for in their respective provided plasmid sequences. Portions of the known plasmid sequences not present in any of the reads were likely due to reads that did not extend long enough to overlap with the subsequent staggered read, not necessarily because the plasmids were missing a portion of their expected sequence. These portions that were unaccounted for were also either small enough or in locations that likely would not significantly impact expression of crucial elements contained in

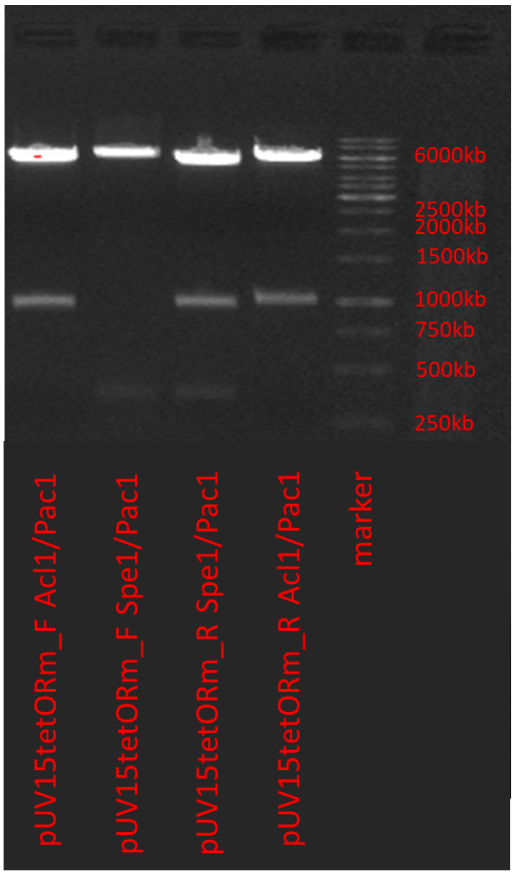

		Size of Gene Products (kb)	
		Acl1/Pac1 digest	Spe1/Pac1 digest
Plasmid	pUV15tetORm_F	1000bp 5968bp	387bp 6552bp
	pUV15tetORm_R	351bp 977bp 5602bp	1000bp 5926bp

Figure 10 Diagnostic digest of pUV15tetORm_F and pUV15tetORm_R plasmids Diagnostic digest of pUV15tetORm_F (lanes 1 and 2) and pUV15tetORm_R (lanes 3 and 4) plasmid backbones. The table indicates expected sizes of bands based on plasmid size and restriction enzymes utilized.

the plasmids. Therefore, we concluded that the pUV15tetORm_F and pUV15tetORm_R plasmids were indeed the actual pUV15tetORm_F and pUV15tetORm_R plasmids and may be utilized as such. Instead of using an empty vector control, *gfp* was chosen for insertion into the plasmid backbones as a control gene due to the added benefit of easy visual confirmation of expression both *in vitro* and *in vivo*. In addition, use of this gene as a control in the tet_{on} system has been previously validated [67]. *gfp* and rel_{Mtb}D81A were PCR-amplified from the pUV15tetORm and pET15b/Rel$_{Mtb}$D81A plasmids, respectively, using the primers listed in Table 1 and inserted separately into the pUV15tetORm_F and pUV15tetORm_R plasmid backbones by molecular cloning. Insertion of these genes was confirmed by a modified form of colony PCR using the same primers referenced above and visualization of DNA bands between 500kb and 750k or 2000kb and 2500kb for *gfp* and rel_{Mtb}, respectively (Figure 11). Gene insertion was also confirmed by Sanger sequencing using the primers listed in Table 3 followed by BLAST analysis against the *gfp* genetic sequence from the pUV15tetORm plasmid, a gift from Sabine Ehrt (Addgene plasmid #17975) [66], and the Tuberculist rel_{Mtb} genetic sequence [62]. These plasmids with their respective gene insertions were designated pUV15tetORm_FGFP, pUV15tetORm_RGFP, and pUV15tetORm_FRel$_{Mtb}$D81A.

Electroporation of plasmids into *Mycobacterium smegmatis*

M. smegmatis is a nonpathogenic, rapidly growing species of *Mycobacteria* frequently used as a surrogate for *M. tuberculosis*. It produces a bifunctional Rel protein capable of synthesizing and hydrolyzing (p)ppGpp [54] and required for survival in stressed conditions [68]. Because of these similarities between *M. tuberculosis* and *M. smegmatis*, phenotypes observed in the two bacteria often mirror each other. Taking advantage of these qualities, initial

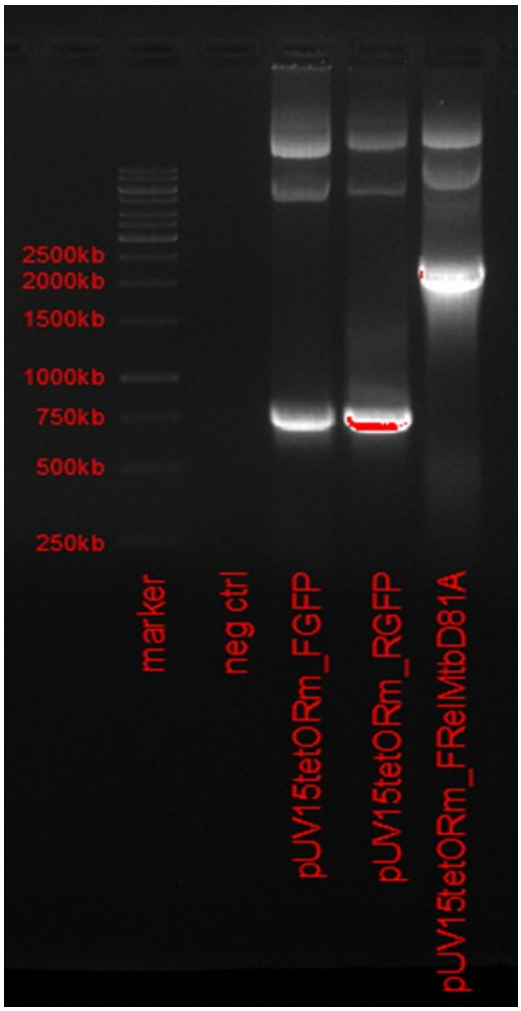

Figure 12 Confirmation of *gfp* and *rel*$_{Mtb}$D81A insertion into plasmid backbones by PCR Agarose gel electrophoresis of PCR products from pUV15tetORm_FGFP (*gfp*, lane 3), pUV15tetORm_RGFP (*gfp*, lane 4), and pUV15tetORm_FRel$_{Mtb}$D81A (*rel*$_{Mtb}$, lane 5) and confirmation of the gene insertion of interest by visualization of the appropriate size DNA band.

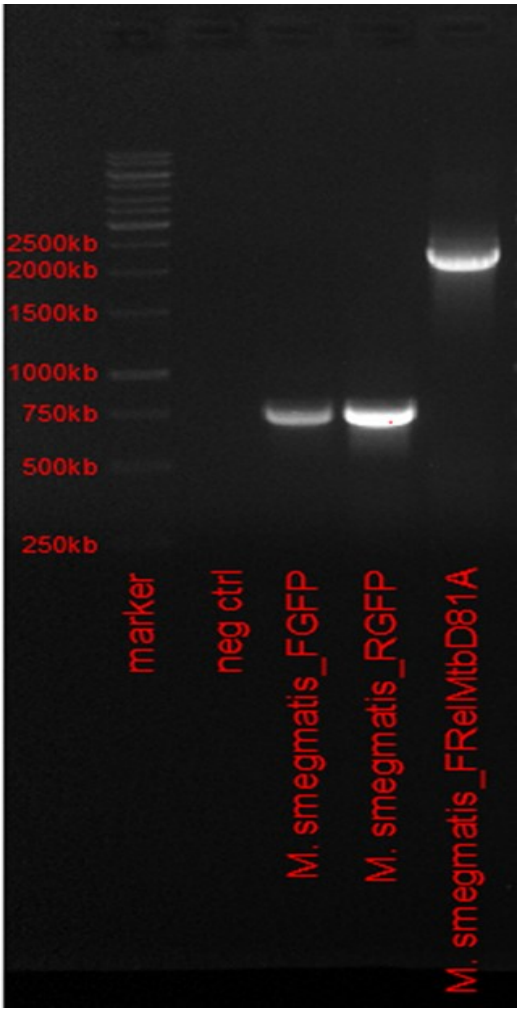

Figure 11 Confirmation of *gfp* and *rel*$_{Mtb}$D81A integration into the *M. smegmatis* genome by PCR Agarose gel electrophoresis of PCR products from *M. smegmatis*_FGFP (*gfp*, lane 3), *M. smegmatis*_RGFP (*gfp*, lane 4), and *M. smegmatis*_FRel$_{Mtb}$D81A (rel$_{Mtb}$, lane 5) and confirmation of the gene insertion of interest by visualization of the appropriate size DNA band.

experiments were performed in *M. smegmatis* as proof of concept for pursuing further studies in *M tuberculosis*. pUV15tetORm_FGFP, pUV15tetORm_RGFP, and pUV15tetORm_FRel$_{Mtb}$D81A plasmids were transformed into *M. smegmatis* by electroporation and plated on 7H10 plates containing hygromycin (50µg/mL). Single colony isolates were selected after incubation for four days at 37°C and their respective gene integrations confirmed by colony PCR (Figure 12) and

Sanger sequencing using the primers listed in Tables 1 and 3, respectively. The resulting strains were designated *M. smegmatis*_FGFP, *M. smegmatis*_RGFP, and *M. smegmatis*_FRel$_{Mtb}$D81A.

qPCR

In order to confirm induced genetic expression of the genes of interest, a time course was conducted and gene expression measured by qPCR at various time points over three days. Expression of *rel$_{Mtb}$* in *M. smegmatis*_FRel$_{Mtb}$D81A increased gradually to a maximum of just over ten-fold 48 hours after induction with the anhydrotetracycline inducer (Figure 13A). Negative controls remained at very low levels or were undetermined.

Western blot

In order to confirm expression at the protein level, a time course was conducted and protein expression measured by western blot at various time points over three days. Confirmation of the specificity of the Rel$_{Mtb}$ antibody was of particular importance considering the presence of Rel$_{Msm}$ in the strains utilized for this experiment. Therefore, the 24 hour, 48 hour, and 72 hour time points for both *M. smegmatis*_FGFP and *M. smegmatis*_FRel$_{Mtb}$D81A were probed with Rel$_{Mtb}$ antibody, revealing a protein band at approximately 75kd in *M. smegmatis*_FGFP samples. Though the presence of this 75kd protein band in *M. smegmatis*_FGFP samples indicated nonspecific binding of the antibody, an additional protein band in the *M. smegmatis*_FRel$_{Mtb}$D81A samples at the expected weight of approximately 82kd restored confidence in the utility of the antibody to accurately distinguish Rel$_{Mtb}$ (Figure 13B). Upon additional probing with the Rel$_{Mtb}$ antibody, expression of Rel$_{Mtb}$ in *M. smegmatis*_FRel$_{Mtb}$D81A was found to gradually increase up to 72 hours after introduction of the inducer (Figure 13C). Samples from time points preceding 12 hours did not contain enough

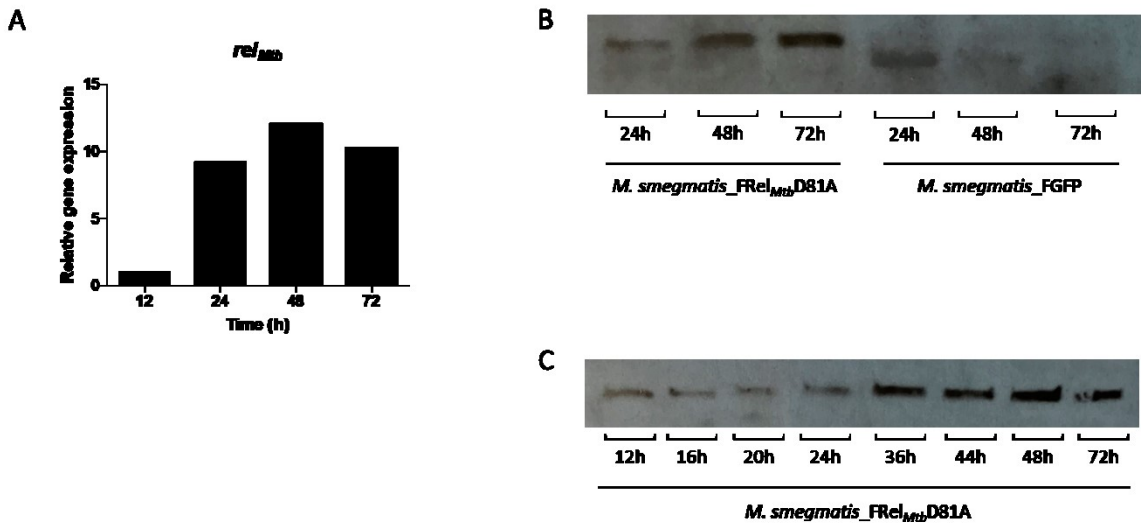

Figure 13 Anhydrotetracycline induction of gene and protein expression Confirmation of inducible expression over time by RT-PCR (A) and immunoblot (B, C) A) rel_{Mtb} gene expression at select time points after induction with anhydrotetracycline in a 72 hour time course. B) Confirmation of antibody specificity for Rel_{Mtb} by probing *M. smegmatis*_$FRel_{Mtb}$D81A (lanes 1-3) and *M. smegmatis*_FGFP (lanes 4-6) protein samples with Rel_{Mtb} antibody at select time points in a 72 hour time course. C) Rel_{Mtb} protein expression after induction with anhydrotetracycline in a 72 hour time course.

detectable protein to allow for loading of reasonable volumes of sample in a gel and were thus excluded.

Growth kinetics

To assess differences in growth rate between *M. smegmatis*_FGFP and *M. smegmatis*_ $FRel_{Mtb}$D81A a growth curve was generated from OD measurements collected during the time course previously mentioned (Figure 14). This growth curve did not illuminate differences in growth kinetics between the two strains in question.

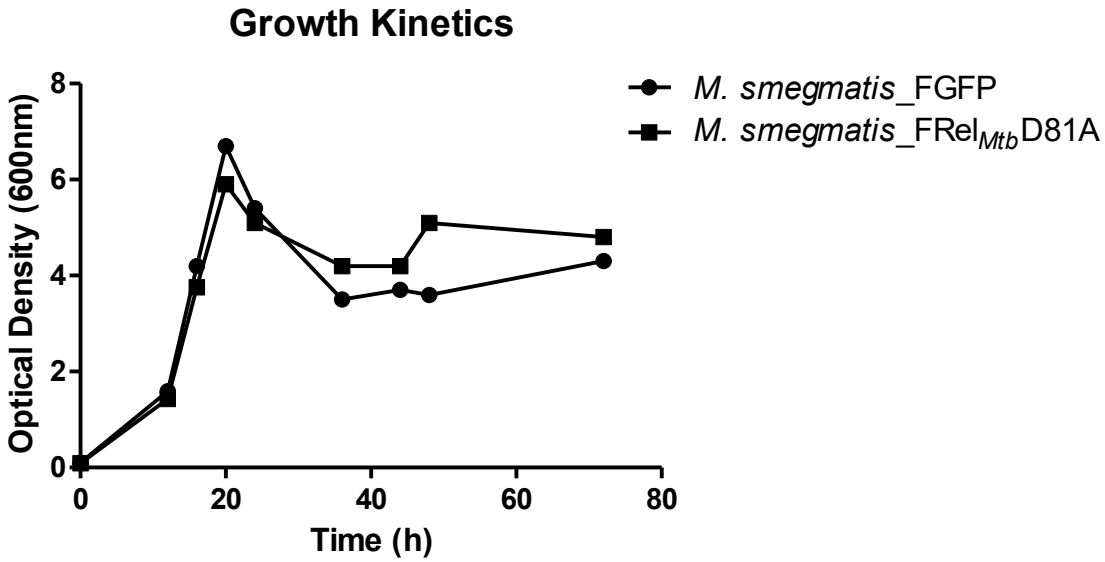

Figure 14 Growth kinetics Growth kinetics of *M. smegmatis*_FGFP and *M. smegmatis*_FRel$_{Mtb}$D81A after induction with anhydrotetracycline in a 72 hour time course

Discussion

Mycobacterium tuberculosis is a pathogenic microorganism causing tuberculosis, a disease that has prevailed as one of the top killers worldwide and was responsible for almost two million deaths in 2016 [4]. The extended six-month duration of treatment for antibiotic sensitive TB complicates effective completion of treatment regimens and is thought to be the result of a small population of nonreplicating, persistent bacteria. Strategies to disrupt this population of bacteria are needed in order to more efficiently kill *M. tuberculosis* and shorten the duration of treatment, hopefully aiding in the eventual elimination of TB.

Persistent *M. tuberculosis* employs the stringent response pathway as a method of reducing replication and metabolic activity to withstand killing by antibiotics without the necessity of possessing a genetic mutation causing antibiotic resistance. The effector molecule of this pathway is (p)ppGpp, whose maintenance within the bacterial cell is controlled by the bifunctional enzyme Rel$_{Mtb}$. There is optimism that learning how to control Rel$_{Mtb}$ function may

enable modulation of the stringent response. With the capacity to influence whether or not *M. tuberculosis* transitions to a persistent state arises the opportunity to drive the bacteria into a more uniform population of replicating microorganisms. This continuity could give current first-line antibiotics affecting replicating bacteria, such as isoniazid, the power to more efficiently target a homogeneous population of bacteria they are more equipped to confront as opposed to struggling against a heterogenous population containing bacteria they are not optimized to kill.

Rel knockout strains have been characterized and much knowledge acquired about its role in bacterial growth and the stringent response. A complementary approach to gain additional insight into the mechanism of this enzyme and its utility in driving advantageous phenotypic changes is creation of a Rel_{Mtb} knock-in strain capable of inducing the stringent response and increasing (p)ppGpp levels in the absence of nutrient deprivation. Generation of this overexpression strain has been accomplished by introducing a point mutation into the Rel_{Mtb} gene at a location known to disrupt (p)ppGpp hydrolysis function and placing the gene under control of an inducible promoter. In this manner, temporal Rel_{Mtb}D81A expression can be controlled and (p)ppGpp synthesis function remains intact to allow accumulation of this alarmone and induction of the stringent response. A rel_{Mtb}D81A gene in the forward orientation with respect to the genome and its corresponding GFP control gene have been integrated into separate *M. smegmatis* genomes and inducible expression of Rel_{Mtb} confirmed at the genetic and protein level. This strain is currently available for further functional characterization.

A growth curve measuring bacterial growth kinetics in the *M. smegmatis*_FRel_{Mtb}D81A strain revealed no difference in growth rate between this strain and its respective control strain. This finding was initially unexpected because rising (p)ppGpp levels and induction of the stringent response would anticipate an early plateau and entrance into stationary phase before

the control strain. However, this growth curve was constructed based on optical density measurements, which do not always reflect changes in viability and can be deceiving due to effects from stress induced changes in the bacterial cell wall on distortion of light refraction. In addition, previous observation of an undesirable *in vivo* phenotype for the control pUV15tetORm_F backbone utilized to create the forward orientation *M. smegmatis*_FGFP strain was the rationale for generating a second, reverse orientation strain. The *in vivo* findings of this forward orientation backbone may explain the seeming lack of a phenotype *in vitro*. It is feasible that both the *M. smegmatis*_FGFP and *M. smegmatis*_FRel$_{Mtb}$D81A strains display a phenotype that is unrecognizable without inclusion of the parental *M. smegmatis* strain excluding integration of the pUV15tetORm_F plasmid. Conversely, other groups have reported the lack of an effect on viability in a Rel$_{Msm}$ knockout strain of *M. smegmatis* [69], but reduced survival in a competition assay against the wild type strain [68], with both groups reporting data using a more accurate measure of CFU counts. In light of these conflicting positions, future functional characterization of the forward orientation strain should include the parent *M. smegmatis* strain and a growth curve based on more reliable CFU counts should be constructed to address the issues presented by questionable viability and effects of cell wall distortion inherent in utilization of the optical density technique. Another possible reason for a lack of difference in growth rate is the presence of native Rel$_{Msm}$. There is no reason to believe Rel$_{Msm}$ would discriminate against (p)ppGpp made by Rel$_{Mtb}$D81A. It is conceivable that while Rel$_{Mtb}$D81A should make increasing amounts of (p)ppGpp without hydrolyzing it, this product is being hydrolyzed by fully functional Rel$_{Msm}$ as quickly as it is synthesized, resulting in a net effect of zero.

In addition to confirming inducible expression of Rel$_{Mtb}$ in the reverse orientation strain, further functional characterization of both the forward and reverse orientation Rel$_{Mtb}$D81A

strains is warranted. Measurement of (p)ppGpp levels using high-performance liquid chromatography (HPLC) or P^{32} radioactive labeled nucleotides and thin layer chromatography would be informative in understanding the effects of eliminating Rel_{Mtb} hydrolysis function and confirm that Rel_{Mtb} overexpression is sufficient to induce the stringent response. Alternatively, poly(P) levels typically rise with increasing (p)ppGpp levels and can be utilized as a simpler, though indirect, measure of (p)ppGpp synthesis. With the increased presence of (p)ppGpp and induction of the stringent response, a diminished growth rate and premature entrance into stationary phase in the Rel_{Mtb}D81A strain before its GFP control counterpart is hypothesized. However, another question concerning the effect of (p)ppGpp overexpression relates to bacterial viability under an excessive stringent response. To address whether or not bacteria enter a dormant state or die due to toxic levels of (p)ppGpp exposure, performing a bacterial viability assay would aid in gaining valuable knowledge regarding the difference between live and dead populations of bacteria during growth. A replication clock assay [70] in which retention of a replication clock plasmid is measured over the course of twenty-one days may also assist in elucidating useful information about bacterial growth rates. This assay makes use of natural plasmid loss in the absence of antibiotic pressure and plating on agar plates with and without antibiotics to reveal the portion of bacteria that retain the replication clock plasmid and enables calculation of the rate at which bacteria replicate. As high retention of plasmid indicates a slower replication rate, and low plasmid retention signifies a faster replication rate, one would expect the Rel_{Mtb}D81A strains to retain more plasmid than the controls due to increased (p)ppGpp, induction of the stringent response, and inhibition of replication. Importantly, the effects of (p)ppGpp accumulation on antibiotic efficacy should be tested. When bacteria are exposed to increasing concentrations of antibiotic in a minimum bactericidal concentration (MBC) assay, the concentration of antibiotic necessary to cause a 2 $\log_{10}$ CFU (99%) reduction of

bacteria is considered the MBC of the antibiotic. Of particular interest is the efficiency of the first-line therapeutic isoniazid in killing the Rel_{Mtb}D81A strains. Because Rel_{Mtb}D81A strains are predicted to increase (p)ppGpp levels and induce the stringent response in nutrient rich conditions, they are expected to display phenotypic tolerance to isoniazid. Thus, the MBC of isoniazid should be higher than that required for wild type *M. smegmatis* in nutrient rich conditions. Furthermore, the plasmid constructs generated in this study may also be utilized to extend exploration of growth and antibiotic tolerance phenotypes to *M. tuberculosis*. In these studies, it would be advantageous to exploit the availability of the *Δrel*$_{Mtb}$ strain of *M. tuberculosis*, as this would eliminate effects potentially caused by background Rel_{Mtb} expression.

Use of small molecule inhibitors of Rel_{Mtb} may also be beneficial in modulating the stringent response to phenocopy *Δrel*$_{Mtb}$ strains. The potential of these small molecules to elicit beneficial phenotypes is an exciting advancement, as they may be optimized and manufactured as medications. With Rel_{Mtb} as a prospective druggable target, innovative ways of shortening TB treatment regimens by targeting the persistent population of nonreplicating bacteria may be possible, placing us one step closer to treating people more effectively and eliminating TB from the world.

Funding

This thesis work would not have been possible without funding from the National Institutes of Health (R21AI122922 and R21AI114507) and the Emergent BioSolutions Fellowship form Emergent BioSolutions Incorporated.

References

1. Iseman MD. A clinician's guide to tuberculosis. Philadelphia: Lippincott Williams & Wilkins; 2000.

2. Centers for Disease Control. Historical Data, 1900-1998. . 2015.

3. Dormandy T. The White Death: A History of Tuberculosis. New York: New York University Press; 2000.

4. World Health Organization. Global Tuberculosis Report 2017. . 2017.

5. World Health Organization. The End TB Strategy. . 2016.

6. Bynum H. Riding the waves: optimism and realism in the treatment of TB. Lancet. 2012;380: 1465-1466.

7. Gunther G, Lange C, Alexandru S, Altet N, Avsar K, Bang D, et al. Treatment outcomes in multidrug-resistant tuberculosis. N Engl J Med. 2016;375: 1103-1105.

8. De Kruif P. Microbe hunters. New York: Harcourt, Brace and company; 1926.

9. Reed RS, Murray EGD, Smith NR. Bergey's Manual of Determinative Bacteriology (7th ed.). 7th ed. Baltimore: The Williams & Wilkins Company; 1957.

10. Ranzani OT, Rodrigues LC, Waldman EA, Carvalho CRR. Estimating the impact of tuberculosis anatomical classification on treatment outcomes: A patient and surveillance perspective analysis. PLoS One. 2017;12: e0187585.

11. Dannenberg AM,Jr. Delayed-type hypersensitivity and cell-mediated immunity in the pathogenesis of tuberculosis. Immunol Today. 1991;12: 228-233.

12. Rohde K, Yates RM, Purdy GE, Russell DG. *Mycobacterium tuberculosis* and the environment within the phagosome. Immunol Rev. 2007;219: 37-54.

13. Ramakrishnan L. Revisiting the role of the granuloma in tuberculosis. Nat Rev Immunol. 2012;12: 352-366.

14. Russell DG, Cardona PJ, Kim MJ, Allain S, Altare F. Foamy macrophages and the progression of the human tuberculosis granuloma. Nat Immunol. 2009;10: 943-948.

15. Wolf AJ, Linas B, Trevejo-Nunez GJ, Kincaid E, Tamura T, Takatsu K, et al. *Mycobacterium tuberculosis* infects dendritic cells with high frequency and impairs their function in vivo. J Immunol. 2007;179: 2509-2519.

16. Schreiber HA, Harding JS, Hunt O, Altamirano CJ, Hulseberg PD, Stewart D, et al. Inflammatory dendritic cells migrate in and out of transplanted chronic mycobacterial granulomas in mice. J Clin Invest. 2011;121: 3902-3913.

17. Davis JM, Ramakrishnan L. The role of the granuloma in expansion and dissemination of early tuberculous infection. Cell. 2009;136: 37-49.

18. Brauner A, Fridman O, Gefen O, Balaban NQ. Distinguishing between resistance, tolerance and persistence to antibiotic treatment. Nat Rev Microbiol. 2016;14: 320-330.

19. Dutta NK, Karakousis PC. Latent tuberculosis infection: myths, models, and molecular mechanisms. Microbiol Mol Biol Rev. 2014;78: 343-371.

20. McDERMOTT W. Microbial persistence. Yale J Biol Med. 1958;30: 257-291.

21. Mitchison DA. The action of antituberculosis drugs in short-course chemotherapy. Tubercle. 1985;66: 219-225.

22. Nuermberger E, Bishai WR, Grosset JH. Latent tuberculosis infection. Semin Respir Crit Care Med. 2004;25: 317-336.

23. Neyrolles O, Hernandez-Pando R, Pietri-Rouxel F, Fornes P, Tailleux L, Barrios Payan JA, et al. Is adipose tissue a place for *Mycobacterium tuberculosis* persistence? PLoS One. 2006;1: e43.

24. Barrios-Payan J, Saqui-Salces M, Jeyanathan M, Alcantara-Vazquez A, Castanon-Arreola M, Rook G, et al. Extrapulmonary locations of *Mycobacterium tuberculosis* DNA during latent infection. J Infect Dis. 2012;206: 1194-1205.

25. Smeulders MJ, Keer J, Speight RA, Williams HD. Adaptation of *Mycobacterium smegmatis* to stationary phase. J Bacteriol. 1999;181: 270-283.

26. Yik Wang C. An experimental study of latent tuberculosis. The Lancet. 1916;188: 417-419. doi: https://doi.org/10.1016/S0140-6736(00)58936-3.

27. Lillebaek T, Dirksen A, Baess I, Strunge B, Thomsen V, Andersen AB. Molecular evidence of endogenous reactivation of *Mycobacterium tuberculosis* after 33 years of latent infection. The Journal of Infectious Diseases. 2002;185: 401-404.

28. Primm TP, Andersen SJ, Mizrahi V, Avarbock D, Rubin H, Barry CE,3rd. The stringent response of *Mycobacterium tuberculosis* is required for long-term survival. J Bacteriol. 2000;182: 4889-4898.

29. Neidhardt FC, Curtiss R. *Escherichia coli* and *Salmonella* : cellular and molecular biology. Washington, D.C.: ASM Press; 1996.

30. Ochi K, Kandala JC, Freese E. Initiation of *Bacillus subtilis* sporulation by the stringent response to partial amino acid deprivation. J Biol Chem. 1981;256: 6866-6875.

31. Braeken K, Moris M, Daniels R, Vanderleyden J, Michiels J. New horizons for (p)ppGpp in bacterial and plant physiology. Trends Microbiol. 2006;14: 45-54.

32. Avarbock D, Salem J, Li LS, Wang ZM, Rubin H. Cloning and characterization of a bifunctional RelA/SpoT homologue from *Mycobacterium tuberculosis*. Gene. 1999;233: 261-269.

33. Cashel M. The control of ribonucleic acid synthesis in *Escherichia coli.* IV. Relevance of unusual phosphorylated compounds from amino acid-starved stringent strains. J Biol Chem. 1969;244: 3133-3141.

34. Artsimovitch I, Patlan V, Sekine S, Vassylyeva MN, Hosaka T, Ochi K, et al. Structural basis for transcription regulation by alarmone ppGpp. Cell. 2004;117: 299-310.

35. Fiil NP, Willumsen BM, Friesen JD, von Meyenburg K. Interaction of alleles of the relA, relC and spoT genes in *Escherichia coli*: analysis of the interconversion of GTP, ppGpp and pppGpp. Molecular & General Genetics: MGG. 1977;150: 87.

36. Chatterji D, Fujita N, Ishihama A. The mediator for stringent control, ppGpp, binds to the beta-subunit of *Escherichia coli* RNA polymerase. Genes Cells. 1998;3: 279-287.

37. Webb C, Moreno M, Wilmes-Riesenberg M, Curtiss R,3rd, Foster JW. Effects of DksA and ClpP protease on sigma S production and virulence in *Salmonella typhimurium*. Mol Microbiol. 1999;34: 112-123.

38. Paul BJ, Barker MM, Ross W, Schneider DA, Webb C, Foster JW, et al. DksA: a critical component of the transcription initiation machinery that potentiates the regulation of rRNA promoters by ppGpp and the initiating NTP. Cell. 2004;118: 311-322.

39. Perederina A, Svetlov V, Vassylyeva MN, Tahirov TH, Yokoyama S, Artsimovitch I, et al. Regulation through the secondary channel--structural framework for ppGpp-DksA synergism during transcription. Cell. 2004;118: 297-309.

40. Mead PS, Griffin PM. *Escherichia coli* O157:H7. Lancet. 1998;352: 1207-1212.

41. Haseltine WA, Block R, Gilbert W, Weber K. MSI and MSII made on ribosome in idling step of protein synthesis. Nature. 1972;238: 381-384.

42. Sajish M, Tiwari D, Rananaware D, Nandicoori VK, Prakash B. A charge reversal differentiates (p)ppGpp synthesis by monofunctional and bifunctional Rel proteins. J Biol Chem. 2007;282: 34977-34983.

43. Xiao H, Kalman M, Ikehara K, Zemel S, Glaser G, Cashel M. Residual guanosine 3',5'-bispyrophosphate synthetic activity of relA null mutants can be eliminated by spoT null mutations. J Biol Chem. 1991;266: 5980-5990.

44. Johnson GS, Adler CR, Collins JJ, Court D. Role of the spoT gene product and manganese ion in the metabolism of guanosine 5'-diphosphate 3'-diphosphate in *Escherichia coli*. J Biol Chem. 1979;254: 5483-5487.

45. Haseltine WA, Block R. Synthesis of guanosine tetra- and pentaphosphate requires the presence of a codon-specific, uncharged transfer ribonucleic acid in the acceptor site of ribosomes. Proc Natl Acad Sci U S A. 1973;70: 1564-1568.

46. Brown A, Fernandez IS, Gordiyenko Y, Ramakrishnan V. Ribosome-dependent activation of stringent control. Nature. 2016;534: 277-280.

47. Sun J, Hesketh A, Bibb M. Functional analysis of relA and rshA, two relA/spoT homologues of *Streptomyces coelicolor* A3(2). J Bacteriol. 2001;183: 3488-3498.

48. Avarbock A, Avarbock D, Teh JS, Buckstein M, Wang ZM, Rubin H. Functional regulation of the opposing (p)ppGpp synthetase/hydrolase activities of RelMtb from *Mycobacterium tuberculosis*. Biochemistry. 2005;44: 9913-9923.

49. Avarbock D, Avarbock A, Rubin H. Differential regulation of opposing RelMtb activities by the aminoacylation state of a tRNA.ribosome.mRNA.RelMtb complex. Biochemistry. 2000;39: 11640-11648.

50. Hogg T, Mechold U, Malke H, Cashel M, Hilgenfeld R. Conformational antagonism between opposing active sites in a bifunctional RelA/SpoT homolog modulates (p)ppGpp metabolism during the stringent response [corrected. Cell. 2004;117: 57-68.

51. Jain V, Saleem-Batcha R, China A, Chatterji D. Molecular dissection of the mycobacterial stringent response protein Rel. Protein Sci. 2006;15: 1449-1464.

52. Jain V, Saleem-Batcha R, Chatterji D. Synthesis and hydrolysis of pppGpp in mycobacteria: a ligand mediated conformational switch in Rel. Biophys Chem. 2007;127: 41-50.

53. Ekal L, Ganesh B, Joshi H, Lama D, Jain V. Evidence of a conserved intrinsically disordered region in the C-terminus of the stringent response protein Rel from mycobacteria. FEBS Lett. 2014;588: 1839-1849.

54. Syal K, Joshi H, Chatterji D, Jain V. Novel pppGpp binding site at the C-terminal region of the Rel enzyme from *Mycobacterium smegmatis*. FEBS J. 2015;282: 3773-3785.

55. Sureka K, Dey S, Datta P, Singh AK, Dasgupta A, Rodrigue S, et al. Polyphosphate kinase is involved in stress-induced mprAB-sigE-rel signalling in mycobacteria. Mol Microbiol. 2007;65: 261-276.

56. Rao NN, Kornberg A. Inorganic polyphosphate supports resistance and survival of stationary-phase *Escherichia coli*. J Bacteriol. 1996;178: 1394-1400.

57. Dahl JL, Kraus CN, Boshoff HI, Doan B, Foley K, Avarbock D, et al. The role of Rel_{Mtb}-mediated adaptation to stationary phase in long-term persistence of *Mycobacterium tuberculosis* in mice. Proc Natl Acad Sci U S A. 2003;100: 10026-10031.

58. Klinkenberg LG, Lee JH, Bishai WR, Karakousis PC. The stringent response is required for full virulence of *Mycobacterium tuberculosis* in guinea pigs. J Infect Dis. 2010;202: 1397-1404.

59. Larsen MH. Some Common Methods in Mycobacteria Genetics. In: Hatfull GF, Jacobs Jr WR, editor. Molecular Genetics of Mycobacteria. Washington, D.C.: ASM Press; 2000. pp. 363.

60. Gandotra S, Schnappinger D, Monteleone M, Hillen W, Ehrt S. In vivo gene silencing identifies the *Mycobacterium tuberculosis* proteasome as essential for the bacteria to persist in mice. Nat Med. 2007;13: 1515-1520.

61. Kapopoulou A, Lew JM, Cole ST. The MycoBrowser portal: a comprehensive and manually annotated resource for mycobacterial genomes. Tuberculosis (Edinb). 2011;Jan 91(1):8-13.

62. Gossen M, Bujard H. Tight control of gene expression in mammalian cells by tetracycline-responsive promoters. Proc Natl Acad Sci U S A. 1992;89: 5547-5551.

63. Gossen M, Freundlieb S, Bender G, Muller G, Hillen W, Bujard H. Transcriptional activation by tetracyclines in mammalian cells. Science. 1995;268: 1766-1769.

64. Lee MH, Pascopella L, Jacobs WR,Jr, Hatfull GF. Site-specific integration of mycobacteriophage L5: integration-proficient vectors for *Mycobacterium smegmatis*, *Mycobacterium tuberculosis*, and bacille Calmette-Guerin. Proc Natl Acad Sci U S A. 1991;88: 3111-3115.

65. Guo XV, Monteleone M, Klotzsche M, Kamionka A, Hillen W, Braunstein M, et al. Silencing *Mycobacterium smegmatis* by using tetracycline repressors. J Bacteriol. 2007;189: 4614-4623.

66. Chuang YM, Bandyopadhyay N, Rifat D, Rubin H, Bader JS, Karakousis PC. Deficiency of the novel exopolyphosphatase Rv1026/PPX2 leads to metabolic downshift and altered cell wall permeability in *Mycobacterium tuberculosis*. MBio. 2015;6: e02428-14.

67. Gandotra S, Schnappinger D, Monteleone M, Hillen W, Ehrt S. In vivo gene silencing identifies the *Mycobacterium tuberculosis* proteasome as essential for the bacteria to persist in mice. Nat Med. 2007;13: 1515-1520.

68. Dahl JL, Arora K, Boshoff HI, Whiteford DC, Pacheco SA, Walsh OJ, et al. The relA homolog of *Mycobacterium smegmatis* affects cell appearance, viability, and gene expression. J Bacteriol. 2005;187: 2439-2447.

69. Wu ML, Chan CL, Dick T. Rel Is Required for Morphogenesis of Resting Cells in *Mycobacterium smegmatis*. Front Microbiol. 2016;7: 1390.

70. Gill WP, Harik NS, Whiddon MR, Liao RP, Mittler JE, Sherman DR. A replication clock for *Mycobacterium tuberculosis*. Nat Med. 2009;15: 211-214.

71. [Anonymous]. Normal chest x-ray. . 2018. Available: https://radiopaedia.org/cases/normal-chest-x-ray.

72. Dannenberg AM,Jr. Perspectives on clinical and preclinical testing of new tuberculosis vaccines. Clin Microbiol Rev. 2010;23: 781-794.

73. Singal B, Balakrishna AM, Nartey W, Manimekalai MSS, Jeyakanthan J, Gruber G. Crystallographic and solution structure of the N-terminal domain of the Rel protein from *Mycobacterium tuberculosis*. FEBS Lett. 2017;591: 2323-2337.

74. Herchline, TE and Amorosa, JK. Tuberculosis (TB) Workup. . 2017. Available: http://emedicine.medscape.com/article/230802-workup#c12.

75. Ponten F, Jirstrom K, Uhlen M. The Human Protein Atlas - a tool for pathology. J Pathol. 2008;216: 387-393.

76. Cambier CJ, Falkow S, Ramakrishnan L. Host evasion and exploitation schemes of *Mycobacterium tuberculosis*. Cell. 2014;159: 1497-1509.

77. Leong FJ, Dartois V, Dick T. A Color Atlas of Comparative Pathology of Pulmonary Tuberculosis. New York: CRC Press; 2011.

Appendix A

Table 1 Primers for PCR amplification, site-directed mutagenesis, and qPCR

Primer Name		Sequence	Purpose	Annealing Temperature
rel$_{Mtb}$ F + Nde1	Forward primer	5' - ACGTCATATGACCGCCCAGCGCAGC ACCACCAAT - 3'	Amplification of *rel*$_{Mtb}$ H37Rv for insertion into pET15b	72°F
rel$_{Mtb}$ F + BamH1	Reverse primer	5’ - ACGTGGATCCCTACGCGGCCGAGGT CACCCGGTA - 3’		
rel$_{Mtb}$D81A SDM	Forward primer	5’ - CGCTGCTGCACGCCACCGTCGAGGA - 3’	SDM introduction of hydrolysis-eliminating point mutation	78°F
	Reverse primer	5' - TCCTCGACGGTGGCGTGCAGCAGC G - 3'		
gfp F + Pac1	Forward primer	5' - AATGAGCACGATCCGCATGCTTAAT ATGGCTAGCCAAGGAGAAG - 3'	Amplification of *gfp* for insertion into pUV15tetORm_F	65°F
gfp R + Acl1	Reverse primer	5' - TACTTTCGATGCTGACAAACGAACG TTATTTGTAGAGCTCATCCATG - 3'		
gfp F + Pac1	Forward primer	5' - AATGAGCACGATCCGCATGCTTAAT ATGGCTAGCCAAGGAGAAG - 3'	Amplification of *gfp* for insertion into pUV15tetORm_R	65°F
gfp R + Spe1	Reverse primer	5' - GGCCGATTCATTAATGCAGCTAGAA TTATTTGTAGAGCTCATCCATG - 3'		
rel$_{Mtb}$ F + Pac1	Forward primer	5' - ACGTTTAATTAAATGACCGCCCAGC GCAGCACCACCAAT - 3'	Amplification of *rel*$_{Mtb}$D81A for insertion into pUV15tetORm_F	69°F
rel$_{Mtb}$ R + Acl1	Reverse primer	5' - ACGTAACGTTCTACGCGGCCGAGGT CACCCGGTA - 3'		
rel$_{Mtb}$ F + Pac1	Forward primer	5' - ACGTTTAATTAAATGACCGCCCAGC GCAGCACCACCAAT - 3'	Amplification of *rel*$_{Mtb}$D81A for insertion into pUV15tetORm_R	69°F
rel$_{Mtb}$ R + Spe1	Reverse primer	5' - ACGTACTAGTCTACGCGGCCGAGGT CACCCGGTA - 3'		

mysA qPCR	Forward primer	5' - TACAAGTTCTCGACCTACGC - 3'	qPCR	54°F
	Reverse primer	5' - AGCTTGTTGATCACCTCGAC - 3'		
gfp qPCR	Forward primer	5' - TGCACTACTGGAAAACTACC - 3'	qPCR	54°F
	Reverse primer	5' - GGATAACGGGAAAAGCATTG - 3'		
rel_{Mtb} qPCR	Forward primer	5' - CCCGGTGAGTTCTTGGAATC - 3'	qPCR	54°F
	Reverse primer	5' - CCTTGGGGGTAAACACGAAA - 3'		

Table 2 Restriction enzymes for gene insertions and diagnostic digests

Restriction Enzyme	Sequence	Purpose
Pac1	5' - TTAATTAA - 3'	Gene insertion, diagnostic digest
Acl1	5' - AACGTT - 3'	Gene insertion, diagnostic digest
Spe1	5' - ACTAGT - 3'	Gene insertion, diagnostic digest
Nde1	5' - CATATG - 3'	Gene insertion, diagnostic digest
BamH1	5' - GGATCC - 3'	Gene insertion, diagnostic digest
HindIII	5' - AAGCTT - 3'	Diagnostic digest

Table 3 Sequencing primers

Primer Name	Sequence	Purpose
rel_{Mtb} F2	5' - CGGGAGATCTATCCCAAGG - 3'	Confirm complete insertion of rel_{Mtb}; confirm hydrolysis-eliminating point mutation
rel_{Mtb} F6	5' - GTGCATTCGCTATGGCAG - 3'	Confirm complete insertion of rel_{Mtb}
rel_{Mtb} F8	5' - GGTTTTCACGTCCAAGGC - 3'	Confirm complete insertion of rel_{Mtb}

rel$_{Mtb}$ F10	5' - AAGCTGGCCAAGTGCT - 3'	Confirm complete insertion of *rel*$_{Mtb}$
rel$_{Mtb}$ R1	5' - AGGTCGGCCTTGGGATAG - 3'	Confirm complete insertion of *rel*$_{Mtb}$
gfp F1	5' - AAACGGCCACAAGTTCAG - 3'	Confirm complete insertion of *gfp*
gfp F2	5' - ACTTCTTCAAGTCCGCCA - 3'	Confirm complete insertion of *gfp*
gfp F3	5' - GAGTACAACTACAACAGCCA - 3'	Confirm complete insertion of *gfp*
gfp F4	5' - AACGAGAAGCGCGATCACAT - 3'	Confirm complete insertion of *gfp*
gfp R1	5' - CTGAACTTGTGGCCGTTT - 3'	Confirm complete insertion of *gfp*
pUV15tetORm_F F1	5' - CGGGAGAACTCCCTATCAG - 3'	Confirm genetic sequence of pUV15tetORm_F plasmid
pUV15tetORm_F F2	5' - GACAGTGTGGTCATCGTTC - 3'	Confirm genetic sequence of pUV15tetORm_F plasmid
pUV15tetORm_F F3	5' - GTCATCGCAAAGAAAACGTC - 3'	Confirm genetic sequence of pUV15tetORm_F plasmid
pUV15tetORm_F F4	5' - GCCGGTCAAGATAGGTTTTT - 3'	Confirm genetic sequence of pUV15tetORm_F plasmid
pUV15tetORm_F F5	5' - GACCTACGACAACAAGATGG - 3'	Confirm genetic sequence of pUV15tetORm_F plasmid
pUV15tetORm_F F6	5' - TGAGATCTTCGAGCACTACC - 3'	Confirm genetic sequence of pUV15tetORm_F plasmid
pUV15tetORm_F F7	5' - ATGAAGGACCGTACGAAGAT - 3'	Confirm genetic sequence of pUV15tetORm_F plasmid
pUV15tetORm_F F8	5' - ATGTAGAGCTGGTCGTTGTA - 3'	Confirm genetic sequence of pUV15tetORm_F plasmid
pUV15tetORm_F F9	5' - GTTTCGTGTGGTTGCTAGAT - 3'	Confirm genetic sequence of pUV15tetORm_F plasmid
pUV15tetORm_F F10	5' - AAATATTGGATCGTCGCACC - 3'	Confirm genetic sequence of pUV15tetORm_F plasmid
pUV15tetORm_F F11	5' - AGGTCGGAATCGAAGGTTTA - 3'	Confirm genetic sequence of pUV15tetORm_F plasmid
pUV15tetORm_F F12	5' - CAGAGCCAGCCTTCTTATTC - 3'	Confirm genetic sequence of pUV15tetORm_F plasmid
pUV15tetORm_F F13	5' - CAGGTCCACGAAGATGTTG - 3'	Confirm genetic sequence of pUV15tetORm_F plasmid
pUV15tetORm_F F14	5' - CCGAACAGCTTGATCACC - 3'	Confirm genetic sequence of pUV15tetORm_F plasmid
pUV15tetORm_F F15	5' - TGGTAACTGTCAGACCAAGT - 3'	Confirm genetic sequence of pUV15tetORm_F plasmid
pUV15tetORm_F F16	5' - GTGAGTTTTCGTTCCACTGA - 3'	Confirm genetic sequence of pUV15tetORm_F plasmid

pUV15tetORm_F F17	5' - TACAGCGTGAGCTATGAGAA - 3'	Confirm genetic sequence of pUV15tetORm_F plasmid
pUV15tetORm_F R1	5' - CTGATAGGGAGTTCTCCCG - 3'	Confirm genetic sequence of pUV15tetORm_F plasmid
pUV15tetORm_R F1	5' - GTACCAACTCGATTCGCTT - 3'	Confirm genetic sequence of pUV15tetORm_R plasmid
pUV15tetORm_R F2	5' - GAACGATGACCACACTGTC - 3'	Confirm genetic sequence of pUV15tetORm_R plasmid
pUV15tetORm_R F3	5' - GTCGAAATGATGTATGCCGT - 3'	Confirm genetic sequence of pUV15tetORm_R plasmid
pUV15tetORm_R F4	5' - GCCGGTCAAGATAGGTTTTT - 3'	Confirm genetic sequence of pUV15tetORm_R plasmid
pUV15tetORm_R F5	5' - GACCTACGACAACAAGATGG - 3'	Confirm genetic sequence of pUV15tetORm_R plasmid
pUV15tetORm_R F6	5' - TGAGATCTTCGAGCACTACC - 3'	Confirm genetic sequence of pUV15tetORm_R plasmid
pUV15tetORm_R F7	5' - ATGAAGGACCGTACGAAGAT - 3'	Confirm genetic sequence of pUV15tetORm_R plasmid
pUV15tetORm_R F8	5' - ATGTAGAGCTGGTCGTTGTA - 3'	Confirm genetic sequence of pUV15tetORm_R plasmid
pUV15tetORm_R F9	5' - GTTTCGTGTGGTTGCTAGAT - 3'	Confirm genetic sequence of pUV15tetORm_R plasmid
pUV15tetORm_R F10	5' - AAATATTGGATCGTCGCACC - 3'	Confirm genetic sequence of pUV15tetORm_R plasmid
pUV15tetORm_R F11	5' - AGGTCGGAATCGAAGGTTTA - 3'	Confirm genetic sequence of pUV15tetORm_R plasmid
pUV15tetORm_R F12	5' - CAGAGCCAGCCTTCTTATTC - 3'	Confirm genetic sequence of pUV15tetORm_R plasmid
pUV15tetORm_R F13	5' - CAGGTCCACGAAGATGTTG - 3'	Confirm genetic sequence of pUV15tetORm_R plasmid
pUV15tetORm_R F14	5' - CCGAACAGCTTGATCACC - 3'	Confirm genetic sequence of pUV15tetORm_R plasmid
pUV15tetORm_R F15	5' - TGGTAACTGTCAGACCAAGT - 3'	Confirm genetic sequence of pUV15tetORm_R plasmid
pUV15tetORm_R F16	5' - GTGAGTTTTCGTTCCACTGA - 3'	Confirm genetic sequence of pUV15tetORm_R plasmid
pUV15tetORm_R F17	5' - TACAGCGTGAGCTATGAGAA - 3'	Confirm genetic sequence of pUV15tetORm_R plasmid
pUV15tetORm_R R1	5' - AAGCGAATCGAGTTGGTAC - 3'	Confirm genetic sequence of pUV15tetORm_R plasmid

Alysha Ellison
422 S. Washington St. Baltimore, Maryland 21231 · (765) 702-9721 · aelliso8@jhmi.edu

Education

Johns Hopkins University, Baltimore, MD
Master of Science in Molecular Microbiology and Immunology
Thesis Title: Generation and characterization of a rel_{Mtb} knock-in strain of *Mycobacterium tuberculosis*
Expected graduation date May 2018
Advisor: Dr. Petros Karakousis

Ball State University, Muncie, IN
Bachelor of Science, May 2015
Major: Premedical Preparation - Biology (Concentration in Microbiology)
Minor: Chemistry

Awards

Emergent BioSolutions Fellowship – Johns Hopkins University, Department of Molecular Microbiology and Immunology (June 2017)

Robert H. and Esther L. Cooper Award – Ball State University, Department of Biology (April 2015)

Sigma Xi Outstanding Undergraduate Student Presentation – Detection of Heat and Acid Stressed *Escherichia coli* O157:H7 in Infant Milk Formula Using Selective/Nonselective Agar Overlays, Ball State University Student Research Symposium (April 2012)

Alpha Lambda Delta Spring 2012 Scholarship Recipient – Alpha Lambda Delta National Academic Honors Society for Freshmen (April 2012)

Dean's Honor List – Ball State University, College of Sciences and Humanities (December 2011 – December 2012; December 2014 – May 2015)

Presidential Scholarship – Ball State University (August 2011 – May 2015)

Employment

Department of Modern Languages and Classics, Ball State University, Muncie, IN
Student Secretary, June 2011 – July 2015

Research Experience

Master's Thesis – Exploring the role of the stringent response in *Mycobacterium tuberculosis* dormancy (January 2017 – Present)
Assess the role of rel_{Mtb} and (p)ppGpp in bacterial growth and the *Mycobacterium tuberculosis* stringent response by creating and characterizing a rel_{Mtb} knock-in strain capable of maintaining continual induction of the stringent response due to synthesis of (p)ppGpp without subsequent hydrolysis.

Research Intern – Eli Lilly and Company, Diabetes Discovery Biology (August 2015 – August 2016)
Performed *in vitro* and *in vivo* experiments exploring the biology of novel targets as potential insulin sensitizers with a focus on adipose tissue and liver. Responsibilities included generation and analysis of data, documentation of experiments in an electronic record keeping database, and interpretation and presentation of data at team meetings.

Undergraduate Research – Ball State University, Department of Biology
Recovery and Enumeration of *Staphylococcus aureus*
Exploratory investigation to develop a time efficient method of enumerating *S. aureus* that is both sensitive and selective in the clinical arena.

Biofilms of Thermoduric *Bacillus* spp.
Preliminary inquiry into the growth and quantification of *Bacillus amyloliquefaciens* biofilms on a microtiter plate in a laboratory setting.

Assessment of GFP-expressing *Bacillus* spp.
Transformation of a previously constructed recombinant plasmid into *Bacillus cereus* bacterial cells, confirmation of the presence of this plasmid in bacterial cells *via* real-time PCR, and plasmid purification.

Genotyping of Enterotoxigenic *Bacillus* spp. Using MVLST
Optimization of genotypic based differentiation and identification of *Bacillus cereus* group isolates using quantitative real-time PCR to identify the presence of target genes.

Microbial Epigenetics in Soil
Isolation and amplification of a known DNA source using quantitative real-time PCR as a control for unknown strains of bacteria found in soil.

Enumeration of Sublethally Injured *E. coli* O157:H7
Presided over project conducted to discover the most effective method and type of media for enumeration of sublethally injured *E. coli* O157:H7 in an infant milk formula food system.

Publications

Bange, J.S., Brumfield, E., **Ellison, A.L.** 2016. Recovery and enumeration of *Staphylococcus aureus* by the selective agar overlay method. *Fine Focus*. 2(1):51-59.

Smith, A.R., **Ellison, A.L.**, Robinson, A.L., Drake, M.A., McDowell, S.A., Mitchell, J.K., Gerard, P., and McKillip, J.L. 2013. Enumeration of sublethally injured *Escherichia coli* O157:H7 ATCC 43895 and *Escherichia coli* Strain B-41560 using selective agar overlays versus commercial methods. *J Food Prot*. 76(4):674-9. doi: 10.4315/0362-028X.JFP-12-363.

Presentations (* denotes presenter)

Bange, J.S., Brumfield, E., **Ellison, A.L.*** 2015. *Recovery and enumeration of* Staphylococcus aureus *by the selective agar overlay method*. Mid-East Honors Association Annual Conference.

Ellison, A.L.*, Bange, J.S. 2015. *Fine Focus: An International Microbiology Journal for Undergraduate Research*. Mid-East Honors Association Annual Conference.

Ellison, A.L.*, Bormann, C.M., Shelton, S.L. 2014. *Fine Focus: An International Microbiology Journal for Undergraduate Research*. Invited talk at Indiana University, Bloomington campus, Bloomington, IN.

Ellison, A.L.*, Cipolla, A. 2014. *Fine Focus: An International Microbiology Journal for Undergraduate Research*. Sigma Xi International Student Research Conference.

Ellison, A.L.*, McKillip, J.L. 2012. *Detection of heat and acid stressed* Escherichia coli *O157:H7 in infant milk formula using selective/nonselective agar overlays*. Indiana Branch of the American Society for Microbiology Annual Meeting and Ball State University Student Research Symposium.

Professional Service

Ad Hoc Manuscript Reviewer
Journal of Dairy Science, 2014 – Present
Fine Focus, 2016 – Present

Secretary, Ball State Chapter of the American Society for Microbiology (BSUASM), August 2014 – May 2015 (Member, August 2010 – May 2015)

Professional Activities/Engagements

Ball State Chapter of Timmy Global Health (Member, August 2012 – May 2015)

Ball State University College of Sciences and Humanities Dean's Student Advisory Council (Member, August 2014 – May 2015)

Community Service

Oneighty Youth Ministries, 4622 N. Broadway Avenue, Muncie, IN
Volunteer, August 2013 – December 2015

Habitat for Humanity, 1923 S. Hoyt Avenue, Muncie, IN
Volunteer, February 2013

Second Harvest Food Bank, 6621 Old State Road 3, Muncie, IN
Volunteer, October 2012

Muncie Mission Ministries, 1725 S. Liberty Street, Muncie, IN
Volunteer, February 2012

References available upon request